UNPUBLISHED PRELIMINARY DATA

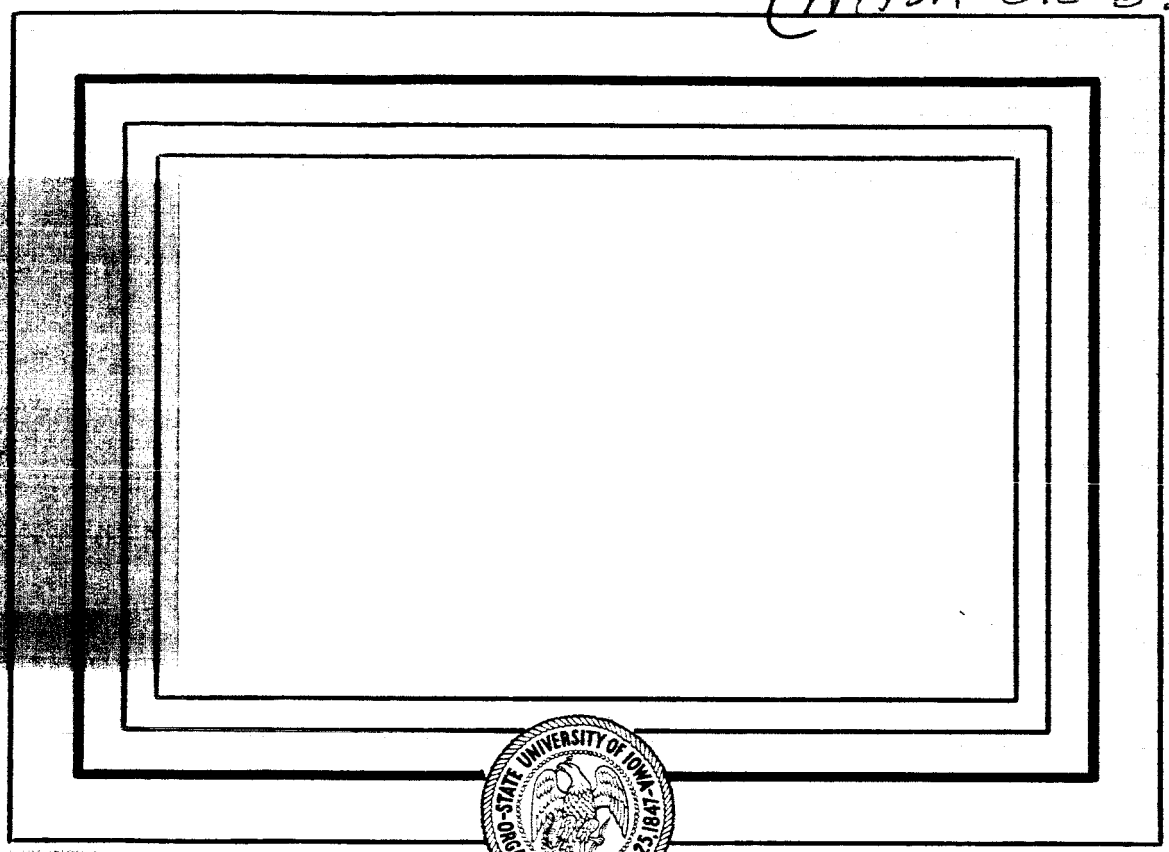

Department of Physics and Astronomy

STATE UNIVERSITY OF IOWA

Iowa City, Iowa

HIGH-LATITUDE GEOPHYSICAL STUDIES WITH SATELLITE INJUN III[+]

PART III: PRECIPITATION OF ELECTRONS INTO THE ATMOSPHERE

by

B. J. O'Brien[*] (Rice U.) [1963] refs

SU163-31

(NASA CR-;-...) OTS: $

(See cover)

Department of Physics and Astronomy
State University of Iowa
Iowa City, Iowa

[+]Research supported in part under contract N9onr93803 with the Office of Naval Research and under grant NsG-233-62 (NASA-) with the National Aeronautics and Space Administration.

[*]Now at Department of Space Science, Rice University, Houston, Texas.

ABSTRACT

13059

A general analysis is made of the precipitation of electrons with energy $E_e \geq 40$ keV into the atmosphere over North America. Measurements were made principally with three directional Geiger tubes on the magnetically-oriented satellite Injun III. It is shown that the intensity of electrons mirroring at the satellite altitude increases rather than decreases when precipitation occurs, for example, over an aurora. The precipitation process is such that the angular distribution of electrons tends to approach isotropy over the upper hemisphere at the satellite altitude. The flux of electrons with $E_e \geq 40$ keV back-scattered by the atmosphere is about ten percent of the precipitated flux. No events have been found where the upflux exceeded the downflux, and it is concluded that most acceleration processes take place high above the satellite, accelerating electrons preferentially parallel to the magnetic-field lines. It is shown that electrons with $E_e \geq 1$ MeV trapped around $L \sim 4$ are not perturbed when electrons with $E_e \gtrsim 40$ keV are precipitated at the same place, and so it is considered that the precipitation is not caused just by a gross change in the magnetic field producing lowered mirror points. The dependence of precipitation on K_p, local and real time, L, and so on is summarized and the implications discussed.

AUTHOR

INTRODUCTION

The intense fluxes of electrons precipitated into the atmosphere at high latitudes originate in the magnetosphere above an altitude of about 1000 kilometers [see O'Brien, 1962, and review therein]. They possess sufficient kinetic energy to penetrate into the atmosphere to altitudes of order 100 kilometers, where they can produce auroras and other phenomena of interest. The origin or the source of these electrons is not known, and many of their properties have been studied only indirectly from consideration of effects produced by them. With satellite-borne instrumentation, the fluxes can be measured directly.

In this note, based on such measurements with the satellite Injun III, the following properties of these fluxes will be considered:

(a) Their pitch-angle distributions, i.e., the variation of particle flux with respect to the angle (α) between the particle trajectory and the local magnetic field vector $\vec{B}$;

(b) Their intensity as a function of magnetic latitude, local time (or longitude), real (or elapsed) time, geomagnetic disturbance, and so on;

(c) The fraction of precipitated electrons backscattered by the atmosphere;

(d) Their energy spectra; and

(e) Their origin.

The particular problem of the specific relationship of these fluxes to the excitation of auroras is treated in a companion paper [O'Brien and Taylor, 1963, hereafter called Part IV].

An earlier study of precipitation was made [O'Brien, 1962] with a single Geiger tube on the satellite Injun I, which was in a high-inclination orbit at an altitude of about (950 ± 50) kilometers. The satellite was not oriented, and so the axis of this directional detector swung at varying angles to $\vec{B}$. Thus occasionally it measured trapped particles, i.e., those particles with pitch angle $\alpha \sim 90°$, and occasionally it measured precipitated or dumped particles, i.e., those with $\alpha \lesssim \alpha_D$, where α_D is the pitch angle at the satellite altitude of a particle which would mirror at 100-km altitude. For the above Injun I investigations, $\alpha_D \sim 55°$. The results of that study of relevance here were as follows, for electrons with energy $E \geq 40$ keV at 1000-km altitude and high latitudes over North America:

(1) In the quiescent state, most of the electrons had a pitch angle $\alpha = 90° \pm 20°$, and the pitch-angle distribution was symmetric about $\alpha = 90°$ because all the electrons were trapped (see Figure 4 of O'Brien, 1962);

(2) Occasionally the pitch-angle distribution widened to include the dumping cone at α_D, as electrons with $\alpha \lesssim \alpha_D$ spiralled down the field lines to plunge into the atmosphere. The angular distribution then became asymmetric as downflux exceeded upflux. A precise measure of the ratio of downflux to upflux could not be made with the single detector (see Figure 4 of O'Brien, 1962, and associated text);

(3) The <u>average</u> flux of precipitated electrons varied from $j \sim 10^2$ to 10^3 particles cm^{-2} sec^{-1} $sterad^{-1}$ at mid-latitudes ($L = 2$ or $\Lambda = 45°$) to $j \sim 10^5$ around the auroral zone ($4 \lesssim L \lesssim 15$ or $60° \lesssim \Lambda \lesssim 75°$) and then decreased by two to three orders of magnitude closer to the magnetic pole (see Figure 8 of O'Brien, 1962). The precipitated flux at a given location in the auroral regions varied over a range of ten thousand to one, so the concept of any "average" values must be treated with care;

(4) This average outflux was so large that if (a) the source of outer-radiation-zone electrons would be stopped and yet if (b) the average outflux would continue at the same rate, then the outer zone would drain empty of such electrons in a few hours; and

(5) Very great changes occurred in the flux in short periods of time or small distances, and these changes were particularly large in the vicinity of the auroral zone.

In a violently variable phenomenon such as electron precipitation in the auroral regions, it is one function of the experimentalist to determine whether any simplifying summary can describe the observations, even if he doesn't understand why it should do so.

It has, therefore, sometimes been suggested that the electrons trapped in the outer Van Allen belt might provide a convenient source of electrons to be precipitated into the atmosphere. In the most simplified version of this suggestion (the leaky-bucket model) the precipitated electrons would be simply formerly-trapped electrons whose energies were unchanged but whose pitch angles were lessened by an unspecified perturbation. Both satellite [e.g., Van Allen and Lin, 1960; Arnoldy, Hoffman, and Winckler, 1960] and balloon [e.g., Winckler, 1961; Anderson, 1960] experiments showed that there must be some acceleration mechanisms which increase the kinetic energy of electrons residing in or entering into the magnetosphere, but the relation of trapped electrons (as detected by Geiger tubes) and precipitated electrons of comparable energy remained unclear.

From the Injun I studies it was suggested [O'Brien, 1962] "that precipitation occurs principally during the acceleration process and that the precipitated particles are fresh particles." It was further stated: "The outer zone should then be regarded not as a 'leaky bucket' that occasionally

spills out particles to cause auroras but rather as a bucket that catches a little of the splash from the acceleration mechanism. For want of a better phrase, it is a splash catcher."

In order to contrast the two models quoted above, an extremely oversimplified comparison of the two is made in Table I. This comparison will be discussed in this note, and it is presented in this elementary form here simply to establish the terminology for later use. It should also be emphasized here that only electrons with energy $E \gtrsim 40$ keV will be discussed, and furthermore that the existence of an electron with energy below this threshold is not even recognized in the splash-catcher model of Table I [see O'Brien, 1962]. It is not the principal role of this present study to determine whether an individual electron which is detected with $E \gtrsim 40$ keV, had recently an energy of a few electron volts as a constituent of a stream of plasma from the sun, or whether it was for many years of thermal energy and a resident of the magnetosphere of the earth, or even whether it was formerly a Van Allen belt electron with energy of say 10 keV. Clearly determination of the immediate past history of a precipitated electron is of interest, and we will discuss it here, but only after the main analysis of this note.

TABLE I

Simplified Comparison

LEAKY-BUCKET MODEL	SPLASH-CATCHER MODEL
TWO Acceleration mechanisms which:	ONE Acceleration mechanism which:
(1) Create energetic trapped electrons,	(1) Creates energetic electrons, some of which are trapped but most of which are precipitated to cause auroras, etc.
(2) dump them later with no energy change and cause auroras.	
IMPLICATION: Outer-zone electrons are the immediate CAUSE of auroras.	IMPLICATION: Outer-zone electrons are generated (in part) BY whatever is the immediate cause of auroras.
TEST: Outer-zone intensity DECREASES when aurora occurs.	TEST: Outer-zone intensity INCREASES when aurora occurs.

As can be seen from Table I, a test of the splash-catcher model is simply to determine whether the flux of trapped electrons increases when electrons are precipitated. If the over-simplified leaky-bucket model was correct, the intensity of trapped electrons instead would decrease during a precipitation event. From Injun I there was an indication that the first situation prevailed. "However, large fluctuations in space and time of the intensity of the electrons (made) it difficult to evaluate this effect quantitatively when only one detector (was) used" [O'Brien, 1962]. Clearly it was desirable to measure the fluxes of trapped and precipitated electrons at the same place and time. This has now been done with an array of Geiger tubes on the magnetically-oriented satellite Injun III, and we will show in the following that the above prediction of the splash-catcher model is correct for low altitudes of order 1000 km. It will be shown that there is evidence for validity of the model also in the equatorial plane at high altitudes. It is emphasized that the purpose of formulating such a model is simply to facilitate discussion. The full validity and implications of the model must be investigated separately in detail. No attempt is made in this note to set up or discuss theories to explain the observed phenomena.

We draw particular attention to the fact that particle fluxes plotted in every figure in this note are always plotted

on a logarithmic scale. Generally the intensity ranges over a factor of one thousand or more, and sometimes over a factor of a million or more. This variability, which is real, should be borne in mind throughout this study.

EXPERIMENTAL APPARATUS

The satellite Injun III was launched on December 13, 1962 into an orbit with apogee altitude 2785 kilometers, perigee altitude 237 kilometers, inclination 70.4° and period 116 minutes. The satellite is described in detail by O'Brien, Laughlin, and Gurnett [1963] hereafter called Part I. Three features of the satellite are of particular relevance to this note.

(1) Its array of Geiger tubes;

(2) Its magnetic orientation; and

(3) The high temporal resolution of its telemetry and data-handling systems.

Relevant characteristics of the three directional Geiger tubes of interest here are listed in Table II (courtesy L. Frank and J. Craven). The relative orientations of these detectors are shown in Figure 1, which also illustrates the usefulness of the magnetic orientation of the satellite. Briefly, the three oriented detectors permit study of electron fluxes which are trapped or precipitated, or a mixture of both. If the pitch angle (α) between a particle trajectory and the local geomagnetic vector $\vec{B}$ is $\alpha \sim 90°$, then the particle is mirroring at the satellite altitude and it is generally deemed to be trapped. If by contrast $\alpha \sim 0°$ then the (precipitated) particle will plunge straight into the atmosphere where it will experience

TABLE II

Injun III Directional Geiger Tubes

Characteristics	Detector 1	Detector 4	Detector 5
Geometric factor (cm^2 sterad)	(0.6×10^{-2}) $\pm$ 20%	(1.1×10^{-2}) $\pm$ 20%	(5×10^{-2}) $\pm$ 30%
Window thickness	1.2 mg cm^{-2} mica	1.2 mg cm^{-2} mica	1.2 mg cm^{-2} mica
Diameter field of view	26°	26°	86°
Orientation	$\alpha = 90°$	$\alpha = 50°$	$\alpha = 0°$
Prescaling factor	2^3	2^3	2^3

Coulomb scattering and energy loss and most likely be absorbed. There is a range of angles $0° \leq \alpha \leq \alpha_D$ which defines a loss cone such that any particle within it is judged to be precipitated and generally lost from the trapping regions. In this note as before [O'Brien, 1962] the value of α_D at the satellite altitude is the pitch angle of a particle that will tend to mirror at 100 km. The value α_D can be determined at a field strength B from the invariant relation

$$\frac{\sin^2 \alpha_D}{B} = \frac{1}{B_{100\ km}} .$$

The values of α_D and general discussion of this invariant relation and other parameters are presented in Appendix I.

The sampling of the Gieger-counter rates and the selection of data are discussed in Appendix II. Evidence for the experimental validity of the results, including discussion of the exclusion of noisy data from extremely variable phenomena, is presented in Appendix III.

OVERSIMPLIFIED VALIDATION OF THE SPLASH-CATCHER

The leaky-bucket model and the splash-catcher model were compared in Table I. There it was shown that a simple test of the two models would be a measurement of the intensity of electrons trapped on the field line through an aurora. If the leaky-bucket model is valid, then the flux of trapped electrons should decrease as they empty out of the radiation zone and cause the aurora. If the splash-catcher model is valid, then since the flux of precipitated electrons must increase to cause the aurora, so should the flux of trapped particles increase.

It will be useful for subsequent discussion to show here immediately that the second situation prevails, thus validating the splash-catcher model at Injun III altitudes.

The photometers on Injun III can detect an aurora at the base of the field line which guides particles detected at the satellite altitude. A discussion of the auroral observations is given elsewhere in this set of papers /O'Brien and Taylor, 1963/. Here a single example of an auroral observation is used.

In Figure 2 are plotted the fluxes of (1) electrons with $\alpha = 90°$; (2) electrons with $\alpha = 50°$; and (3) light in the spectral region around 3914 Å, for a northbound passage of the satellite at night over North America. At low values of L, the flux of electrons at $\alpha \sim 90°$ is of order one hundred times

greater than the flux of those at $\alpha \sim 50°$. Indeed, most of the electrons measured by Detector 4 at low values of L in this pass were trapped. Only at $L \gtrsim 4$ was the viewing cone of Detector 4 completely inside the dumping cone (see Appendix I). When the satellite reached auroral latitudes, it measured a very large increase in the flux of precipitated electrons, i.e., of those with $\alpha \sim 50°$, and at the same location the intensity of 3914 Å light increased greatly as these and other precipitated particles caused an aurora.

Simultaneously the intensity of trapped electrons with $\alpha = 90°$ increased greatly (see Figure 2) to a flux essentially the same as that of the precipitated electrons. This observation, and many others like it detected by Injun III [see O'Brien and Taylor, 1963] thus validates the splash-catcher model in its comparison with the leaky-bucket model. We may now investigate the extent of the validity of some of the extreme oversimplifications in this splash-catcher model. Note in particular that it has been validated here only at Injun III altitudes of order 1000 kilometers. This does not imply that it is still valid for particles with $\alpha_o \sim 90°$. In order to test it for such particles, data from high-altitude satellites which travel near the equatorial plane must be used.

Clearly for an ideal test of the splash-catcher at high altitudes one should have a satellite measuring directional

fluxes in the equatorial plane, comparing the flux with an equatorial pitch angle $\alpha_o \sim 0°$ and that with $\alpha_o \sim 90°$. This has not yet been done (see Appendix I). So in this note, we consider precipitated electrons measured by Injun III at low altitudes in 1963, and compare them with trapped electrons measured by Explorer XII at high altitudes in the equatorial plane in 1961. The two sets of measurements can therefore be compared only on a statistical basis, and the planetary magnetic index K_p at the time of each measurement is taken as a parameter governing the behavior of each.

From Injun III data of December 1962 through February 1963, the maximum flux of electrons with $E_e \geq 40$ keV precipitated during each high-latitude pass is plotted in Figure 3A against the value of K_p at the time of the pass. Each flux was averaged over 8 seconds (or ~ 50 km of satellite trajectory) in order to smooth over extremely brief fluxes.

From Explorer XII passes in 1961, Freeman [1963] found the maximum counting rate of a given detector on each equatorial pass through the outer zone, and plotted it against K_p at the time (Figure 3B). The plotted counting rates are averages over many spins, and hence are roughly omnidirectional intensities, dominated by locally-trapped particles with $\alpha_o \sim 90°$ [see Rosser, O'Brien, Van Allen, Laughlin, and Frank, 1962]. The

detector measures electrons with $E_e \sim (50 \pm 10)$ keV. In the outer zone these dominate the spectrum with $E_e \geq 40$ keV.

Figures 3A and 3B show that the flux of precipitated and of trapped electrons both increase with K_p. It is also apparent, even with considerable scatter of the data, that the flux of precipitated electrons increases more with increase of K_p than does the flux of those trapped at high altitudes. If we assume that both the increases are due to a common acceleration mechanism, then we can conclude that the acceleration mechanism acts preferentially parallel to $\vec{B}$, but with a finite and lesser effect at larger angles to $\vec{B}$. This is, of course, the prediction of the splash-catcher model [O'Brien, 1962].

The validation of the splash-catcher in the equatorial plane depends on the assumption that the maximum spin-averaged flux in the equatorial plane and the maximum precipitated flux would be seen on the same magnetic field line if simultaneous observations were made. Our present imperfect knowledge of the locus of the field lines (or guiding centers) at large values of L is consistent with this assumption for the above statistical comparison, but the assumption cannot be proved. It is conceivable that the results of Figures 3A and 3B have different causes. It is simpler to assume that they have a common cause and together with Injun III results as in Figure 2 this would imply that the splash-catcher model is valid through the whole of the outer zone.

BACKSCATTERED ELECTRONS

It was found with Injun I that electrons with $E \geq 40$ keV are precipitated, and also that some precipitated electrons are backscattered by the atmosphere [O'Brien, 1962]. However, with only a single, slowly-spinning detector on Injun I sampling highly-variable fluxes it was not possible to measure accurately the ratio of backscattered electrons to precipitated electrons. Such a measurement has now been made with the array of detectors on Injun III.

We define the reflection coefficient (R_α) at a given pitch angle α (where $\alpha \leq 90°$) as the ratio between the directional flux of particles coming upwards from the earth at a given angle to $\vec{B}$ and the directional flux travelling downwards at the same angle. In effect, R_α is the ratio of the directional flux at $(180° - \alpha)$ to the directional flux at (α). Clearly $R_\alpha = 1$ when $\alpha = 90°$ when the Alfvén approximation holds. In order to determine what proportion of dumped particles is actually absorbed in the atmosphere, R must be evaluated over the range $\alpha = 90°$ through $\alpha = \alpha_D$ to $\alpha = 0°$. (Only Northern Hemisphere data are discussed here. In the Southern Hemisphere the same discussion applies if the supplements of all angles are used.)

Such an evaluation can be made theoretically, but it is a complex problem because of the electron gyration around $\vec{B}$,

the non-radial direction of $\vec{B}$ except over the poles, the dependence on the angular distribution of the downflux and so on. (We are indebted to Dr. F. Mozer and Dr. D. Elliott for valuable discussions on this theoretical evaluation.) For the present purposes, we simply make a relatively crude experimental measurement.

Soon after separation the satellite spun with such a large amplitude that all detectors swung over a wide range of α. The parameter R_α can be measured accurately at $\alpha < \alpha_D$ only when intense fluxes of electrons are being precipitated, and it is at just such times and places that the electron fluxes vary so rapidly. Therefore both $j(\alpha)$ and $j(180° - \alpha)$ must be measured at the same time and the same place so as to find R_α.

This has been done using Detectors 1 and 7 on Injun III. Detector 1, a thin-windowed Geiger counter, points in one direction, and the differential spectrometer channel Detector 7 points in the opposite direction. From the early period of spinning and tumbling of the satellite, occasions were chosen when there were intense fluxes of precipitated electrons at high latitudes, and when the above detectors were spinning rapidly through a wide range of α. The value of α is determined from the flux-gate magnetometer whose axis is parallel to those of the above detectors. The magnetic dip was more than 70° in every example chosen for this analysis.

Detectors 1 and 7 are not identical, so that R_α cannot be obtained immediately from their respective counting rates. However, in a given pass and a given spin we can obtain their respective counting rates when they view the same flux at $\alpha = 90°$ (when $R_\alpha = 1$). Suppose the ratio of the counting rate of Detector 1 to that of Detector 7 is X when $\alpha = 90°$. Then suppose that the ratio at another value of α with Detector 1 pointing up, is Y at $\alpha = \alpha_1$, say. Then $R_{\alpha=\alpha_1} = \frac{X}{Y}$. The resultant plot from many spins on six passes is shown in Figure 4. The data were taken from differing locations so that α_D varied as shown.

The above treatment implicitly assumes that the different energy response of Detectors 1 and 7 is unimportant. The fluxes studied were those in which Detectors 7 and 8 and other electron detectors showed that most of the electrons measured by Detector 1 had energies around 40 to 50 keV, and hence were measured equally well by Detectors 1 and 7. In most cases, there were a few counts registered by Detector 8, which views the same direction as Detector 7 but which responds to electrons with energy around 90 keV [see O'Brien, Laughlin, and Gurnett, 1963]. In such examples, the reflection coefficient for these $\sim$ 90 keV electrons was usually slightly less than that of the electrons with energy $\sim$ 50 keV, but the Poissonian errors associated with the small counting rates of Detector 8 were

relatively large, and the data are not regarded as sufficiently definitive to be plotted here. They do show, however, that 90 keV electrons have a finite reflection coefficient comparable with that of 50 keV electrons, and hence they justify the use made here of an integral measurement (by Detector 1) and a differential measurement (by Detector 7) in order to find a reflection coefficient for typical outer-zone electrons with $E \geq 40$ keV.

A direct integral measurement of R_α was made when an intense and brief precipitation event occurred while Detector 1 was pointed down viewing $\alpha = 170°$ electrons and Detector 4, a similar detector, viewed $\alpha = 130°$ and hence trapped particles at this location. From discussion which will follow, it may be seen that in such precipitation events the flux of trapped electrons is about the same as the flux of precipitated electrons. Hence in this case, Detector 1 measured upflux, and Detector 4 may be taken as measuring downflux. The resultant value of R_α plotted in Figure 4 is in good agreement with that obtained from Detectors 1 and 7.

We conclude from Figure 4 that over the dumping cone at high latitudes, the flux of backscattered electrons with $E \geq 40$ keV is about ten percent of the flux of precipitated electrons with $E \geq 40$ keV. This value, which ignores dependence of R_α on energy and pitch angle, is reliable to a factor of better

than two, which is sufficient for our purpose. It would be valuable to have a more accurate measurement, made preferably with identical energy-discriminating detectors with narrow ($\lesssim 5°$ in diameter) fields of view.

Note that in the sixteen measurements made in the dumping or loss cone and plotted in Figure 4, R_α is always less than one. This is in contrast to the rocket observation by McDiarmid, Rose, and Budzinski [1961] of $R_\alpha > 1$, and it shows that such cases are rare. More measurements of R_α with special instruments such as mentioned above would enable one to decide how often angular distributions with $R_\alpha > 1$ occur.

This determination of the reflection coefficient is of relevance in studying conjugate-point phenomena, if it can be shown that the backscattered electrons will be able to travel to the opposite hemisphere. This requires that the local magnetic-field line be sufficiently well-ordered to act as a guiding center. It will be shown below that on at least some occasions this requirement is satisfied. It also requires that a 40-keV electron can travel back up the field line without being essentially stopped by the acceleration mechanism. This and associated problems are discussed below.

SAMPLES OF SPLASHES

In the following studies data principally from January and February, 1963, when the satellite was oriented, are used.

When Injun III was at low values of L, such as $2 \lesssim L \lesssim 4$, the counting rates of Detectors 1, 4, and 5 generally varied smoothly with time or place. At higher values of L, however, in auroral regions, the counting rates of the detectors would sometimes change greatly in a few seconds. A short segment of data from such an occasion is shown in Figure 5, where each detector was sampled about four times each second. It is clear from this figure that when Detector 5 exhibits a marked increase in counting rate, so does Detector 4 and so does Detector 1.

When such examples are sampled at higher rates, this qualitative behavior is still apparent. This is shown in Figure 6, in which the sampling rate was sixteen times each second.

From a pass of Injun III through the auroral regions, many examples of such synchronous changes in these counting rates can usually be observed. For convenience of subsequent discussion, any such event will be called a "splash". As here defined, a splash is an event which is detected by noting that Detector 5 has measured a brief enhancement, and confirmed

by noting that the other detectors measured an enhancement at the same time. It is not defined by examining Detector 1 or Detector 4 first. The significance of this is discussed below.

Because the changes in counting rate in a splash event are synchronous, it may be assumed that they have a common cause.

On the above assumption that the increments of fluxes seen by three detectors have a common cause, and because the precipitated particles must have been generated very recently and could not have been trapped with the same energy and the same pitch angle, we will call each increment of flux at each pitch angle "fresh" particles. By this it is implied that the particles in each increment did not formerly exist at that pitch angle with that energy. It is important to note that if the old particle flux was (as usual) a monotonically-decreasing value with increasing energy above ~ 10 keV, then a mechanism which adds an increment of energy without changing the pitch angle of each particle will give an increase in the flux of electrons with $E_e \geq 40$ keV. Various other conceivable effects could also lead to "fresh" particles, and these are considered below.

TRAPPING DURING PRECIPITATION

An interesting problem is to determine whether trapping can possibly occur on a field line which is the guiding center for a precipitation event. Now the precipitation could be caused by acceleration over part or all of the field line. If it occurred over all of a field line then every electron spiralling around that field line must have encountered the acceleration mechanism. On the other hand, if it occurred over a part of the field line for a time shorter than the bounce period of trapped electrons, then many of the latter would be completely unaffected by it. Because the Geiger-tube counts are accumulated for ~ one quarter (or ~ one sixteenth) of a second, which are times shorter than the bounce periods, it is possible that they do not give a representative sample of the particle population along the entire length of a line of force. It appears to us, however, that the following treatment is independent of any such effects.

There are several numerical values of relevance here /see Van Allen, 1963, for general discussion of periodic motions of trapped particles/. At L ~ 4 and ~ 1000-km altitude, an electron with 50 keV kinetic energy will bounce to-and-fro in latitude in about 1 second, and will drift in longitude so that each successive mirror point in a given hemisphere (say) is

about 2 km to the east of the previous mirror point. Sampling times of the detectors range from about one-sixteenth to one-quarter of a second here. The satellite moves at a speed of about 8 km/sec near perigee and ~ 6 km/sec near apogee. The cyclotron radius of gyration averages about 20 meters over the range of observation here.

We determine whether trapping and precipitation are possible on the same field line at the same time by comparing the behavior of low-energy ($E_e \geq 40$ keV) electrons with that of high-energy ($E_e \gtrsim 1$ MeV) electrons at the same time and place. High-energy electrons are present in large fluxes around $L \sim 3.5$ to 4 [see Laughlin, Fritz, and Stilwell, 1963] and many splashes were observed in that region while Injun III was spinning soon after separation, and also at later times when it was oriented.

Two detectors which measure high-energy electrons are used here. The first, Detector 3, measures electrons with energy $E \gtrsim 250$ keV over the same conical field of view as does Detector 1. The second, Detector 6, is an omnidirectional detector which most efficiently detects penetrating electrons with energy $E \gtrsim 1.5$ MeV. It also responds to bremsstrahlung from lower-energy electrons, but from the other Injun III detectors it can be shown that the bremsstrahlung contribution was negligible in the cases studied here.

Two splashes on two passes are used here. In the first, Detectors 1 and 3 pointed into the dumping cone. Before and after the splash (which occurred over about one second in time or seven kilometers in distance) they detected an electron beam in which

$$j(E \geq 40 \text{ keV}) \sim (3.6 \pm 0.2) \times 10^5 \text{ particles cm}^{-2} \text{ sec}^{-1} \text{ sterad}^{-1}$$
$$j(E \gtrsim 250 \text{ keV}) \sim (6.3 \pm 0.2) \times 10^3 \text{ particles cm}^{-2} \text{ sec}^{-1} \text{ sterad}^{-1}.$$

During the splash, these detectors found

$$j(E \gtrsim 40 \text{ keV}) \sim (14.3 \pm 0.1) \times 10^5 \text{ particles cm}^{-2} \text{ sec}^{-1} \text{ sterad}^{-1}$$
$$j(E \gtrsim 250 \text{ keV}) \sim (11 \pm 1) \times 10^3 \text{ particles cm}^{-2} \text{ sec}^{-1} \text{ sterad}^{-1}$$

where the errors in each case are Poissonian standard deviations derived from the number of counts registered. The absolute accuracy of each measure and the variation of flux within a splash are not of importance here where only relative changes are considered.

Thus the splash produced a fourfold increase in the flux of electrons with $E \geq 40$ keV, and roughly doubled the flux of electrons with $E \geq 250$ keV.

Yet before, during, and after the splash the flux of high-energy ($E \gtrsim 1.5$ MeV) electrons measured by Detector 6 did not change by more than ten percent, and the counting rates are consistent with no change at all. In order to present the fluxes, we assume that Detector 6 measured electrons with

$E \geq 2$ MeV with unity efficiency. Then before and after the splash

$$J\,(E \gtrsim 2 \text{ MeV}) = (120 \pm 6) \text{ particles cm}^{-2} \text{ sec}^{-1}$$

and during the splash

$$J\,(E \gtrsim 2 \text{ MeV}) = (120 \pm 10) \text{ particles cm}^{-2} \text{ sec}^{-1}.$$

Therefore, it appears valid to state that the high-energy ($E \gtrsim 1.5$ MeV) electrons were still trapped and unperturbed on the same field line on which particles were being accelerated. The complete to-and-fro bounce time of such particles at this location was about 0.5 seconds, and the splash lasted for twice this time.

In another splash, a similar analysis showed a ten-fold increase in the precipitated flux of electrons with $E \geq 40$ keV, but less than a twenty percent change and possibly no change, in the flux of electrons with $E \geq 250$ keV and with $E \gtrsim 1.5$ MeV. A number of other examples have also been studied, and in no case has a statistically-significant change in the omnidirectional flux of electrons with $E \gtrsim 1.5$ MeV occurred when a splash occurred. Furthermore, with Detector 20 on Injun III we can also show in each event that the <u>directional</u> intensity of electrons with $E_e \gtrsim 1.3$ MeV trapped at Injun altitudes did not change in the splashes studied. Indeed, we have not yet observed with Injun III what might be called a splash of such

high-energy electrons. (One may have been detected by us with Explorer VII over a visible aurora on November 28, 1959.)

This finding implies that high-energy ($E_e \gtrsim 1$ MeV) electrons can be trapped and unperturbed on a field line along which fresh electrons are being precipitated with energies $E_e \geq 40$ keV. Clearly this finding must be significant in speculations about the acceleration mechanisms causing precipitation. Because this is the first occasion on which this problem has been resolved we consider the implications briefly here. The discussion applies only to the region $L \lesssim 5$, which is the only region in which high-energy ($E_e \gtrsim 1$ MeV) electrons are present in large fluxes.

Some qualitative theories suggest that precipitation is initiated by the introduction of a 'blob' of plasma into a geomagnetic tube of force, whereupon space-charge effects and drifting charges can proceed to affect previously-trapped (Van Allen) particles [e.g., see Chamberlain, 1961b]. If it is assumed that such a blob would result in the complete loss of trapped high-energy ($E_e \sim 1$ MeV) particles in its immediate vicinity without producing a compensating flux of 'fresh' similar particles, then the fluxes of these particles can be used as a probe of the spatial and temporal characteristics of the blob, since they bounce to and fro along the tube. We showed above that there was less than a ten percent change in the directional

or omnidirectional fluxes of high-energy ($E_e \sim 1$ MeV) trapped electrons in the midst of such precipitation. So, on the above working hypothesis, fewer than ten percent of the high-energy electrons in the tube of force would have been exposed to the blob. But they bounce from one hemisphere to the other in only 0.25 seconds, while precipitation persisted for several seconds in the samples studied. So (if we ignore drift in longitude) the high-energy electrons must have passed through the blob some ten times, yet fewer than ten percent (and perhaps none) were lost. It appears, therefore, that if a blob initiated the splash, it must have had such characteristics as to have introduced negligible distortion of the magnetic field lines acting as guiding centers of the high-energy electrons. We do not understand how a blob could have been introduced in the first place without such a distortion occurring. This negligible perturbation of high-energy trapped electrons must be explained by any theories of precipitation.

It has been suggested very often that precipitation may result simply from lowering of mirror points of previously-trapped particles without a change in their energy. Indeed, this is what was formerly meant by "dumping" trapped particles. Most of the mechanics proposed to lower the altitude of mirror points have assumed that the particle motion is such as to endeavor to conserve the invariants /see Van Allen, 1963/

in a distorted geomagnetic field. For example, suppose that the magnetic moment is conserved and that the scalar magnetic field everywhere along the guiding center is decreased. Then the particles formerly mirroring at $B = B_1$ say, will still tend to mirror there, even if B_1 is now deep in the atmosphere. In another treatment, Vestine [1960] considered the geomagnetic field distorted by the solar wind, and particles formerly trapped so that they mirrored just above the appreciable atmosphere on the daytime side of the earth. If the magnetic moment invariant was conserved, then they would still mirror at the same field strength B_1, and in the dipole field of the earth, B_1 is found at lower altitudes if the latitude is lower. If the integral invariant of their motion was conserved, then they would tend to mirror at lower latitudes on the nightside than on the dayside. Hence, according to this treatment trapped particles mirroring just above the atmosphere on the daytime side will be dumped in the atmosphere when they drift in longitude to nighttime side. Several observations [Forbush, Venkatesan, and McIlwain, 1961; Paulikas and Freden, 1963] indicate that particles are trapped at a given location which will mirror in the atmosphere when they drift in longitude even in the unperturbed but non-centered dipole geomagnetic field.

Our results above show that the observed precipitation or splash is not a simple lowering of mirror points of all particles on a given field line. Instead, it is an energy-dependent process, having a great effect on electrons with $E_e \geq 40$ keV but a negligible effect on electrons with $E_e \gtrsim 1$ MeV.

It is interesting to note here that there is other evidence that outer-zone electrons with $E_e \sim 50$ keV behave differently from electrons with $E_e \gtrsim 1$ MeV. For example, the flux of the lower-energy electrons increases during the main phase of a magnetic storm [see Freeman, 1963], while the flux of the higher-energy electrons decreases at first, and then increases a day or so later [see Fan, Meyer, and Simpson, 1960; Farley and Sanders, 1962; also McIlwain, 1963]. Furthermore, the spectral slope of electrons trapped in the outer zone during quiescent conditions appears to be relatively flat for energies below a few hundred keV, but relatively steep above such energies [see Rosser et al., 1962]. One might speculate that precipitation and acceleration of low-energy (~ 50 keV) electrons are caused mostly by electric fields of some tens of kilovolts while the intensity changes in the higher-energy (~ 1 MeV) electrons are caused mainly by gross changes in the magnetic field with betatron acceleration or deceleration [e.g., see Coleman, 1962; McIlwain, 1963] which, with a steeply-falling

energy spectrum, can result in great changes in the flux of electrons of a given large (~ MeV) energy. It should be emphasized that such speculations remain, at present, only speculations.

In the above treatment, it was seen that fluxes of trapped electrons with $E_e \gtrsim 40$ keV are modified during precipitation events. Now this modification is examined in detail, both in specific examples of splashes and in statistical summaries of splashes. The object of this treatment is to attempt to arrive at a common description of the phenomena.

PHENOMENOLOGY OF PRECIPITATION

Measurements of electrons with $E_e \geq 40$ keV on a typical high-latitude ($L \sim 7$) pass are shown in Figure 7. The altitude of this pass was only about 250 kilometers, so that the trapped electrons were mirroring at almost as low an altitude as they can reach without a high probability of suffering Coulomb scattering in a few bounces. Their Southern Hemisphere mirror points in this case were well above 500 km.

Throughout the thirty seconds of data shown, the flux of precipitated electrons increased by a factor of one hundred thrice and by lesser but still significant amounts several times. By contrast, the flux of trapped electrons remained constant to within a factor of two. There were five statistically-significant increases in the trapped flux at the times of large precipitation, but the other variations in the flux at $\alpha \sim 90°$ are not statistically significant. (This can be verified by reference to the geometric factors listed in Table I. Note that the telemetered numbers are the accumulated counts pre-scaled by eight and the resultant discreteness of plotted data also increases the apparent changes in Figure 7.)

In order to discuss these data more fully, angular distributions derived from measurements A and B in Figure 7

are shown in Figure 8. Shown in the same Figure 8 is the angular distribution obtained by subtracting the flux at A from the flux at B. Note that with equal validity one might subtract (instead of A) the flux just after the precipitation event B ends. If that was done the flux of "fresh" particles at $\alpha = 90°$ shown in Figure 8 would be (2.7×10^4) instead of (3.3×10^4) particles cm^{-2} sec^{-1} $sterad^{-1}$, and hence the angular distribution of fresh particles would have even a deeper minimum at $\alpha = 90°$ than is sketched. A similar analysis could be made of any of the other "splashes" in Figure 7. From such analyses the following summaries can be made:

Summary (a): In a precipitation event the precipitation is such that the flux of electrons with $E_e \gtrsim 40$ keV tends to approach isotropy over the upper hemisphere (within the crude angular resolution of the three detectors).

Summary (b): The increment of the flux (i.e., the flux of "fresh" electrons as defined above) roughly parallel to the local magnetic vector $\vec{B}$ is greater than that at right angles to $\vec{B}$.

We now show that these two summary statements are applicable generally to precipitation events or splashes. From about fifty oriented passes over North America early in 1963, many splashes were found by visual scanning of the counting rate of Detector 5. Most of the data was acquired at $L \gtrsim 5$ because most splashes occur there, but there was no deliberate selection

of data with reference to L, altitude, local time, or geomagnetic activity. The data are therefore as random a sample of precipitation as one can obtain with a satellite in a fixed orbit. Splashes of only a few seconds duration or less were chosen so that "increments" of fluxes or fluxes of "fresh" particles could be estimated in the same way as in Figure 8 from Figure 7.

In Figures 9 through 14 scatter diagrams are presented of both the total fluxes and the increments of fluxes in these splashes. Figure 9 illustrates the tendency towards isotropy or summary (a) above. Figure 10 illustrates that the increment of flux or the flux of "fresh" electrons is greater near $\alpha \sim 0°$ than at $\alpha \sim 90°$, or summary (b) above.

Furthermore, Figures 11 and 12 show that the same summaries are valid even if data from Detectors 1 and 4 (viewing $\alpha \sim 90°$ and $\alpha \sim 50°$) are compared. This is particularly significant because a "splash" was defined above by reference to another instrument, Detector 5 viewing $\alpha \sim 0°$, and hence the selection of events was independent of the results of Detectors 1 and 4. For comparison, Figure 13 shows the relative fluxes measured by Detectors 1 and 4 not during splashes but during the period soon after launch when the satellite was spinning and tumbling and when the two detectors viewed the same value of α. Figure 13, therefore, provides a measure of con-

fidence in the calibration of the relative geomagnetic factors of Detectors 1 and 4, and it also shows the scatter of comparative flux measurements by the two detectors (see calibration discussions in Appendix III).

Finally, in Figure 14 the increments of fluxes at $\alpha \sim 50°$ and $\alpha \sim 0°$ are compared. It is seen that often the increments are about the same, but that the increment at $\alpha \sim 50°$ is more often the greater than it is the smaller. This was also the case in the single event analyzed in Figures 7 and 8, although there it was only just significant. From this result, we can derive another summarizing statement, viz.:

Summary (c): During a splash the angular distribution tends to widen over the upper hemisphere, and continues to widen until it is flat, i.e., until the distribution is isotropic over the upper hemisphere.

These three summary statements describe the phenomenology of a "splash" without regard to its cause. The processes that might cause a splash are discussed below, after the general characteristics of precipitation are discussed with respect to its dependence on L, local time, and other significant parameters.

The rocket observations of Davis et al. [1960] and McDiarmid et al. [1961] established that fluxes of electrons tended towards isotropy at the relatively-low altitudes of ~ 120 to ~ 150 kilometers. It may also be noted that Chamberlain

/1961a/ states that an isotropic distribution is "to be expected for particles propelled toward the atmosphere from an injection source or center of acceleration located far above the atmosphere." In his treatment, he assumes (a) an initial isotropic distribution of fresh particles (b) conserving the magnetic moment invariant and then merely traces their trajectories down $\vec{B}$ to the atmosphere. Clearly, our observations of isotropy are necessary for the validity of (a) and (b) but it is not at all clear that they are sufficient to establish their validity. The angular distribution in precipitation widens out in precipitation from the usual narrow distribution of trapped particles (see summary (c) above). An alternative conceivable possibility would be for fresh particles to arrive very strongly peaked parallel to the field line, so that the total angular distribution of "fresh" plus old trapped particles would have a maximum at $\alpha \sim 0°$, another maximum at $\alpha \sim 90°$, and a minimum between. This second possibility does not occur, so that apparently the "fresh" and the trapped electrons are very closely related, and we deduce from this that the increment of trapped electrons and perhaps all the electrons at $\alpha \sim 90°$ with a given energy are "fresh" in the sense that before precipitation occurred these very same electrons did not exist with the same pitch angle and energy.

GENERAL FEATURES OF PRECIPITATION

The features of electron precipitation are now presented for two purposes: First, so that they may be used in ground-based studies of the ionospheric phenomena which they cause; and second, so that it may be clear what features any acceptable theory of the acceleration mechanism (s) must explain. Many of the features presented here are well-known already from studies with x-ray detectors on balloons [e.g., Anderson, 1960; Pfotzer, Emmert, Erbe, Keppler, Hultqvist, and Ortner, 1962; Winckler, 1961; Winckler, Bhavsar, and Anderson, 1962; Brown, Anderson, Anger, and Evans, 1963], and from very many ground-based observations [e.g., Basler, 1963] as well as from previous satellite studies [O'Brien, 1962]. Nevertheless, they are grouped here so as to provide a convenient summary. Each characteristic will be illustrated by a figure from Injun III data. Such figures should not be regarded as typical, but merely as illustrative. All the treatment of this section will be a descriptive catalogue. Discussion of the significance of the findings will follow.

It should be noted by those interested in comparing these data with ionospheric effects, that all of our relevant measurements are made with directional detectors, and hence all measured fluxes are directional fluxes in units of particles

cm^{-2} sec^{-1} $sterad^{-1}$. In order to find the total flux of particles bombarding unit area of the ionosphere, i.e., in order to find the flux in particles cm^{-2} sec^{-1}, these directional fluxes must be summed over 2 π sterad. As has been shown, the flux in precipitation events tends towards isotropy over the upper hemisphere, so that one may reasonably multiply all fluxes quoted here by 2π in order to obtain the flux bombarding 1 cm^2 at 100-km altitude say. The validity of such an action is enhanced by the fact that Detector 5 has a wide field of view ($\sim 43°$ half-angle) so that it effectively measures an average directional flux over much of the dumping cone. In fact it was designed specifically to fill this need at the planned satellite altitude of $\sim$ 950 kilometers. Note also in consideration of ionospheric effects that only some 90% of precipitated electrons are absorbed immediately (see discussion of R_α above).

The properties of precipitated electrons which might be measured are their flux and energy spectrum as a function of

(1) L or invariant latitude Λ ;

(2) Local time;

(3) Real time; and

(4) Pitch angle.

The simplest feature to measure, and that which can be measured with highest sensitivity and greatest accuracy, with Injun III, is the directional flux of precipitated electrons with energy

$E_e \geq 40$ keV, and this is considered first. This flux has been measured with Detector 5 for all North American passes in January and February, 1963 and for favorably-oriented portions of passes in December, 1962. Both scatter diagrams from many passes and segments of data from selected passes are used. Much of the data involves eight-second (i.e., thirty-two frame) averages taken at half-integral values of L. Occasionally such short-period averages lie in the middle of a splash, and sometimes they lie just outside a splash. They were chosen to be this short because the satellite takes a comparable time to cross a half-unit of L at high L values. Also, in eight seconds the satellite moves about fifty kilometers, and this is about the scale of resolution in numerous ground-based observations.

Consider first the precipitation as a function of L (or invariant latitude Λ) only. Figure 15 shows data from two successive passes of January 14, 1963 separated in real time by two hours. They were at essentially the same local times, and were separated in longitude by about thirty degrees. No attempt has been made to show the fine structure in these latitude profiles, although samples of the range of fluctuation of intensities are shown. The plotted points are eight-second (i.e., thirty-two sample) averages at half-integral values of L.

Figure 15 illustrates two features. It shows that precipitation can be very restricted in latitude (e.g., over Δ L ~ 1 earth radius) or very extensive in latitude (e.g., over

$\Delta L \sim 20$ earth radii) even at the same local time and over an interval of only a few hours in real time. A comparable variability was found in the latitude survey by x-ray detectors on balloons [cf. Winckler et al., 1962]. The second feature to be noted in Figure 15 is that considerable precipitation occurred in one pass even at L values as large as about 30, corresponding to an invariant latitude of about 80°.

Considering further the precipitation as a function of L only, a scatter diagram for precipitation during January, 1963 is shown in Figure 16. Data from other months are not plotted, so as to avoid too complex a figure.

Figure 16 illustrates two features of interest. First, it shows that precipitation is roughly one thousand times larger in the auroral region than it is at mid-latitudes around $L \sim 2$. This can be seen by the line representing the average of the measurements in Figure 16, and of course, it is clear how a few very intense fluxes can dominate such an average. The average latitude profile is in good agreement with that derived from Injun I [O'Brien, 1962] with considerably fewer measurements. The significance of this profile in considerations of the concept of particle "lifetime" was discussed by O'Brien [1962] and the discussion will not be repeated here, except to mention that quantitatively the Injun III measurements confirm the accuracy of those with Injun I but show the scatter of the

phenomenon more fully. A second feature of Figure 16 which should be noted is that the flux of precipitated electrons at a given value of L in the auroral zone can vary over a range of at least a million to one. Hence the source at a given location is not continuously very active even in the auroral zone. The significance of this will be discussed below, and here it is sufficient to mention that, by contrast, the solar wind (a suggested source of energy for precipitation) does blow continuously /Neugebauer and Snyder, 1962/. Note however that the minimum outflux over the range L = 5.0, 5.5, ..., 7.0 out of 241 measurements (not all on different passes) is about 40 particles cm^{-2} sec^{-1} $sterad^{-1}$, significantly higher than at other values of L. Precipitation therefore occurred all the time near the auroral zone, but at a slightly lower latitude than the auroral zone which was defined by photometric measurements of auroral light to be around L = 7.8 (see Part IV). Basler /1963/ found auroral ionospheric absorption also to be at lower latitude than the visual auroral zone, and so presumably the absorption he studied was caused more by electrons with $E_e \geq 40$ keV than by electrons with $E_e \sim 10$ keV.

In continuing this presentation of the L-dependence of precipitation, it is useful to compare Figures 17 and 18, which show short segments of data from a pass on January 13, 1963. In Figure 17, the precipitation is essentially constant to

within about 10% for more than ten seconds, or about one hundred kilometers in distance. In Figure 18, by contrast, the precipitation is greatly variable in short times and/or small distances. More extreme examples of each feature can be found in other passes, ranging from a hundred-fold increase and decrease in the flux in less than one-quarter of a second(or in about two kilometers), to the other extreme of continuous precipitation constant to about 10% for a time of about twenty seconds. The two examples compared here were chosen simply because they were acquired about two minutes apart on the same pass.

Precipitation may also be studied as a function of local time. Recent studies at low altitudes with Injun I [O'Brien, 1963] and at high altitudes with Explorer XIV [Frank, Van Allen, and Macagno, 1963] show that the location in the magnetosphere of geomagnetically-trapped radiation is influenced by the angle between the sun-earth vector and the earth-location vector. The data can be organized with, and display a systematic dependence on, the parameter local time. It is of interest to see if the fluxes of precipitated electrons show a similar dependence.

Again we use both individual events and scatter diagrams of many events. Individual events used are those in which telemetry was received on both the northbound and southbound portions of a pass of Injun III over North America. Two

contrasting events are considered, and these are shown in Figures 19 and 20.

It is clear from Figure 19 that the precipitated flux at 1930 U.T. on January 13, 1963 was more dependent on L than on local time, and indeed the fluxes at the same L (L = 7.5 say) separated in local time by about five hours (or about seventy-five degrees of longitude) and in real time by about seven minutes are remarkably similar. Because they are so similar, it is reasonable to assume that the flux extended over the entire width of 75° longitude. From this assumption, and from the measured dependence of precipitated flux on L, we find a total instantaneous power input of electrons $E \geq 40$ keV into the Northern Hemisphere of about three hundred megawatts. In different units, the total energy input of these particles over at least five minutes was 10^{18} ergs. When electrons with energy $E_e \geq 1$ keV are included, if use is made of the equivalence relation often applicable to such electron fluxes that when

$$j\ (E_e \geq 40 \text{ keV}) \sim 10^5 \text{ particles cm}^{-2} \text{ sec}^{-1} \text{ sterad}^{-1}$$

then $j\ (E_e \gtrsim 1 \text{ keV}) \sim 1 \text{ erg cm}^{-2} \text{ sec}^{-1} \text{ sterad}^{-1}$ [see O'Brien, 1962], we find the instantaneous energy flux precipitated for at least five minutes was $\sim 10^{18}$ ergs/sec. The significance of these numbers will be discussed below when the requisite source strength is calculated.

The data of Figure 20, by contrast with those of Figure 19, show very different fluxes at the same L shell but different local times. The detailed latitude profile of Figure 20 is seen more clearly in Figure 21. Since the satellite takes a finite time (~ minutes) between crossing an L shell on a northbound pass and next crossing it on a southbound pass, and since the precipitated flux at the same point can vary greatly in a few seconds and even more in a few minutes, the effects in Figure 20 could be due to a variation in real time rather than local time or longitude. We therefore have no evidence from Injun III to show that the flux must on occasions be localized in longitude, and merely present Figure 20 as a contrast to Figure 19 which shows that on occasions the flux must be extended in longitude. Evidence for a longitudinal difference might be inferred from joint Injun I-Explorer XII observations, where Injun I measured at low altitudes the most intense natural event yet seen in space [O'Brien and Laughlin, 1962] while Explorer XII on the same L shell but at high altitude measured an unperturbed outer zone flux at the same time but at a different longitude. Comparison of high-altitude data with low-altitude data in this way is liable to uncertainties because they do not refer to particles with similar equatorial pitch angles, and the matter is not resolved here from consideration of these and other individual events.

So instead we consider scatter diagrams of precipitated flux versus local time from many passes in December, 1962, and January and February, 1963. These are sorted over two ranges of L in Figures 22 and 23. Measurements made on both northbound and southbound portions of a given pass (i.e., roughly at the same real time) are so indicated. The figures show no particular evidence for a systematic local time dependence which we can detect, and we would summarize both Figure 22 and Figure 23 by the statement that both intense and weak precipitation can occur during both the day and the night, both at midday and midnight.

By contrast with precipitated electrons, trapped electrons at 1000-km altitude and high L values show a large, one-hundred fold enhancement during the day over the flux during the night. Compare, for example, Figure 2 of O'Brien [1963] for trapped electrons at $8 \leq L < 10$ with Figure 22 of this study. The difference between the systematic behavior of trapped electrons and the seemingly-unsystematic behavior of precipitated electrons may be summarized by saying that there are generally large fluxes of electrons <u>trapped</u> at 1000-km altitude at $L \sim 8$ during the day, but there are not always large fluxes of <u>precipitated</u> electrons. Consequently there is a very great variation in precipitated flux at a given L and a given local time, and this variation is sufficiently large to obscure in this study any systematic behavior. Ground-based observations

acquiring continuous data for a year or so can settle this matter more satisfactorily than we can here [e.g., see Basler, 1963]. The very great increase in precipitation which occurs during magnetic storms, and the fact that the satellite orbit is fixed in local time for the duration of a storm, make the scatter of Figures 22 and 23 so large.

The next parameter to consider then, is real time or elapsed time. Again the satellite suffers from a disadvantage in studying short-time variations, because while it samples in time it is moving at a speed of some 6 to 8 km/sec, and temporal and spatial variations can rarely be resolved. The balloon measurements of x-rays find intensity changes in times of a second or less [Winckler, 1961] and these must be temporal rather than spatial effects because the atmospheric target area giving the x-rays is ~ 100-km diameter, and this is of course far greater than the drift distance of the balloon in such short intervals. Again, the rockoon measurements show similar rapid changes in intensity [Van Allen, private communication] and although in this instance the target is small and moving, it moves horizontally by only a few cyclotron radii in the period of changing flux.

Here we will concentrate on long-term (~ hours) changes in the precipitated flux. In this case, only a scatter diagram can be used, and in Figure 24 is shown the flux of precipitated

electrons for January 1963. Similar plots have been made for other periods but these are not shown here. Also shown is the planetary magnetic disturbance index K_p. Since K_p refers to an interval of three hours in time, it is relevant to note that the precipitated fluxes plotted are eight-second averages at certain values of L. The short-term flux measurements and the long-term magnetic index may therefore be expected to have a somewhat imperfect relationship.

It is clear from Figure 24, however, that it is reasonable to state that there is a greater tendency to have high fluxes of precipitated electrons during magnetic storms (or large K_p) than at magnetically-quiet times. Such a conclusion is scarcely new, but it is included here for completeness. It is essential to phrase it in such vague terms, because the phenomenon in question displays such erratic behavior.

The index K_p is recognized to be a very crude measure of geomagnetic activity, but it has been used in so many studies that we compare it here with the intensity of precipitation in order to see if it can be given a quantitative evaluation.

The maximum eight-second-average precipitated flux encountered on each pass is plotted against K_p in Figure 3A. This use may be thought of as a measure of the most intense precipitation which a given disturbance can produce, independent of latitude or L. A similar general dependence is seen if one

plots the precipitation at a given L (e.g., L = 6) against K_p.

It is useful to compare the scatter diagram of Figure 3A with a similar diagram compiled by Freeman [1963] of the most intense flux of 50 keV electrons encountered by Explorer XII on passes in the equatorial plane (Figure 3B). The particles measured by Freeman were trapped, and on the average their intensity increased by a factor of ten (with considerable scatter) as K_p increased by five units from 0 to 5. By contrast, Figure 3A here shows that the corresponding increase in precipitated particles is by a factor of more than one thousand, with very great scatter at a given K_p.

This comparison might be summarized by saying that, for K_p between 0 and 5, the maximum (i.e., any L) flux of precipitated electrons with $E_e \geq 40$ keV increases by roughly a factor of about five for every unit increase in K_p. The index K_p is therefore, as generally recognized, fairly crude.

The precipitation pitch-angle distributions can be summarized, as shown above, by the statement that the fluxes in intense precipitation are isotropic over the upper hemisphere just above the appreciable atmosphere, e.g., at ~ 250-km altitude. Furthermore, about ten percent of the precipitated flux is backscattered by the atmosphere, and since it has been shown that the same field lines can occasionally be guiding centers during precipitation, these backscattered electrons may

tend to travel to the conjugate point. Whether they reach the conjugate point will be determined by their ability to pass back through the acceleration region without being decelerated or otherwise perturbed. The simultaneous conjugate-point balloon x-ray studies by Brown, Anderson, Anger, and Evans [1963], show that the intensities of precipitated electrons are essentially the same in both hemispheres, so that presumably the acceleration mechanism operates in both senses, precipitating primary electrons in both hemispheres.

The properties of precipitated electrons with $E_e \geq 40$ keV at high latitudes and Injun III altitudes over North America may be summarized as follows:

(1) The average flux increases from $\sim 10^2$ particles cm^{-2} sec^{-1} $sterad^{-1}$ at L = 2 ($\Lambda = 45°$) to $\sim 10^5$ in the auroral zone L ~ 5 to 10 ($\Lambda \sim 62°$ to 72°) and then decreases again (Figure 16).

(2) The maximum flux over all latitudes and the flux at a given latitude increase by roughly a factor of five with every unit increase in K_p from 0 to 5, varying greatly at any chosen K_p (Figure 3A). The precipitated electrons are much more susceptible to magnetic storms than are trapped electrons (Figure 3A versus Figure 3B).

(3) The precipitated flux on occasions can be uniform over ~ 80° of longitude or > 4000 kilometers (Figure 19). On other

occasions it may be localized in longitude, although this is not proven here (Figures 20 and 21).

(4) The precipitated flux can be extremely extensive in latitude, extending over $\Delta L \sim 20$ "earth radii" and up to about ten degrees from the magnetic pole (Figure 15) or it can be extended over only $\Delta L \sim 1$ earth radius and negligible at high latitudes (Figure 15), and it may extend uniformly over hundreds of kilometers in latitude (Figure 17) or over only a few kilometers (Figure 18).

(5) The precipitated flux can be intense or weak at any time of the day, in particular both at midday and at midnight (Figures 22 and 23).

(6) The angular distribution of the precipitated flux tends towards isotropy over the upper hemisphere (Figures 7 through 14), and

(7) About ten percent of the precipitated flux is backscattered by the atmosphere (Figure 4).

(8) The precipitated flux reaches a maximum value on a given pass at about the same location as any aurora and also at about the boundary of trapping (Figure 2).

ENERGY SPECTRA IN PRECIPITATION

Detailed spectral analyses of precipitated electrons will not be presented here, because such analyses are included in the spectral studies of Laughlin, Fritz, and Stilwell [1967] in Part II. However, a brief summary of observed spectral characteristics will be included here so as to complete the description of the characteristics of precipitation.

It was shown above that the energy spectrum of trapped electrons is much richer in high-energy ($E_e \sim 1$ MeV) electrons than is the spectrum of precipitated electrons (at $L < 5$, where the comparison could be made in small precipitation events).

In the energy range 40 keV $\leq E_e \leq$ 110 keV a few spectral analyses could be made as a function of pitch angle when the differential spectrometer was spinning and tumbling with the satellite soon after launch. No significant variation with pitch angle could be detected.

Another approach is to measure the spectrum in this range when the satellite was oriented, so that the spectrometer detected trapped particles with $\alpha \sim 90°$. A number of large splashes were examined, and the spectrum measured before, during, and after the splash. If the spectrum before and after was essentially the same, it was taken to be a precipitation event of reasonable spectral stability. (This may have produced

a bias in the conclusions we draw here). In such cases, it was found that the spectrum during the splash was essentially the same as before and after. For example, comparing counting rates during one splash of two seconds duration with the rates in the previous ten seconds, the low-energy (~ 50 keV) channel increased by 360% while the high-energy (~ 100 keV) channel increased by 370%. Another method of comparison is to fit an exponential curve to the two-point measurement, numerically integrating over the actual spectral passbands (see Part II). Then in this same event the e-folding energy E_o was found to be

(i)	Before the splash	$E_o = (23.8 \pm 0.5)$ keV
(ii)	During the splash	$E_o = (24.1 \pm 0.5)$ keV
(iii)	After the splash	$E_o = (22 \pm 1)$ keV

The above treatments indicate that the spectrum in the range $40 \leq E_e \leq 110$ keV may be not greatly affected by precipitation. They show that the spectrum in a splash is not strongly dependent on pitch angle (at Injun altitudes) and that the spectrum of trapped particles inside a splash is much the same as it was on either side of (or before and after) the splash. Similar conclusions can be reached from a statistical study of the spectra of trapped and precipitated electrons [see O'Brien, 1962]. It is to be emphasized that they apply as yet only to altitudes of $\lesssim$ 1000 km. The approach to isotropy during precipitation also suggests that this is likely

to be true, since the integral fluxes above 40 keV become roughly equal, and they are composed mostly of electrons with energy $40 \leq E_e \leq 110$ keV.

The variation in spectra from event to event is now treated briefly. Fuller discussion is given in Part II. Several qualitative statements can be made, viz., the spectrum in the range $E_e \leq 100$ keV may be greatly variable with time and/or space in a given event, but it appears to be generally softer towards higher latitudes [see also O'Brien, 1962]. In many precipitation events there is an abundance of electrons with energy $E_e \sim 10$ to 40 keV, and in several events it is certain that the flux of precipitated electrons with $E_e \sim 10$ eV is no larger than the flux of those with $E_e \sim 10$ keV (see Part IV). Thus the energy spectra on some occasions at least do not continue to rise at the same slope down to near-thermal energies. The acceleration mechanism may be such, therefore, as to supply a minimum amount of energy (e.g., ~ 1 keV, say) to any participating electrons [see also McIlwain, 1960; Davis et al., 1960].

ENERGY REQUIRED TO DRIVE PRECIPITATION

One of the first requirements of any postulated source or acceleration mechanism is that it be capable of supplying sufficient energy to keep precipitation going, both on an instantaneous localized basis and on a long-term, world-wide basis. For example, it is often suggested that the solar wind may be the source of energy that leads to the energizing of the outer radiation zone, of precipitation and then auroras. Accurate measurements of the solar wind have now been made [Neugebauer and Snyder, 1962] so that this energy balance may be examined quantitatively.

Briefly, it can be shown by measurement of auroral light (Part IV) and by direct measurement of particle precipitation, that the average energy flux of electrons with $E_e \geq 1$ keV precipitated in the auroral zone is about 3 to 5 ergs cm^{-2} sec^{-1}. When averaged over the planet earth, this corresponds to an average energy loss of (4×10^{17}) ergs sec^{-1}. (Most of this loss occurs in magnetic storms, but the time-averaged conditions are treated here.) The average solar wind brings to the front of the magnetosphere (about 10 R_e in radius) some 3×10^{19} ergs sec^{-1}. Thus if the average solar wind is to drive the average precipitation and thence auroras, a mechanism must be found for converting about one percent of the solar-wind energy.

On some occasions, precipitated fluxes as great as ~ 2000 ergs cm^{-2} sec^{-1} are observed [see McIlwain, 1960; O'Brien and Laughlin, 1962]. If these (or the bright auroras they cause) cover some 10 km in latitude and some 4000 km in longitude as they may, then the instantaneous precipitated energy is of order 10^{18} ergs sec^{-1}. Then if the solar wind is the source of this energy a mechanism must be found to concentrate it and transform it in an appropriate manner, and also to transfer it to the dark as well as the sunlit side of the magnetosphere.

THE CAUSE OF PRECIPITATION

The various characteristics of precipitation of electrons in dynamic high-latitude events were summarized in a preceding section. It should also be noted that Balmer emissions occur in the auroral zone [see Chamberlain, 1961a] and these might well be interpreted as indicating proton precipitation analogous to the above electron precipitation. The localized proton flux apparently can be as large as 10 ergs cm^{-2} sec^{-1} and it may be more widespread than the more intense electron precipitation. It seems possible that similar total amounts of energy might be precipitated by particles of both types, but there are few experimental measurements of protons with $E_p \sim 10$ to 100 keV at satellite altitudes [see Davis and Williamson, 1962]. We ignore protons in the following discussion, but emphasize that this is not to imply that they have negligible effects.

The above comparison of the behavior of high-energy ($E_e \sim 1$ MeV) and low-energy ($E_e \geq 40$ keV) electrons in splashes indicates that this precipitation is not simply a gross lowering of mirror points of all trapped electrons. Instead it is an energy-dependent effect. It must involve the energizing of electrons, because otherwise the outer zone would be rapidly emptied [see detailed discussion by O'Brien, 1962]. Then the

"increment" of energy supply must be of the order of tens of keV or less, rather than say hundreds of keV, in order for its effects on 1 MeV electrons not to be discernible. On the other hand, the increment of energy must be of the order of tens of keV rather than say hundreds of eV, because otherwise the peak flux of auroral electrons would not be found at energies of the order of 10 keV. The differential energy spectrum is steep for $E_e > 40$ keV, but tends generally to flatten or perhaps turn over at energies of a few keV to some 10 keV [see Parts II and IV; McIlwain, 1960; Davis et al., 1960; Anderson and DeWitt, 1963].

It seems possible that a sharp peak at, say, 6 keV in the differential electron spectrum [as in McIlwain, 1960] might be caused simply by thermal electrons in part of the tube of force being exposed to an electrostatic potential of ~ 6 kV, directed along the field vector $\vec{B}$.

There appear to be some features of the precipitation consistent with a crude, qualitative assumption that splashy precipitation is caused by temporary electric fields of the order of 10 kilovolts directed parallel to $\vec{B}$ at high altitudes. However, we have no suggested mechanism for creating such a field, or for determining its characteristics, and there are so many adjustable parameters that we have not yet solved the transport equation which describes the behavior of an electron originally having a given energy at a given pitch angle [see also Chamberlain, 1961b].

It must be remembered that the tendency towards isotropy was established above only at altitudes of ~ 1000 km and less, by detectors with opening angles of tens of degrees, for fluxes of electrons with energy $E_e \geq 40$ keV. It would appear from Figures 3A and 3B that isotropy does not persist in the equatorial plane. If an electric field along $\vec{B}$ causes precipitation then perhaps a flux of electrons ~ 10 keV should have a maximum parallel to B, although obscure scattering phenomena at high altitudes might cause it to approach isotropy at lower altitudes $\ll$ 1000 km. The only occasions on which we find greater fluxes at $\alpha \sim 0°$ and $\alpha \sim 50°$ than at $\alpha \sim 90°$ are for very low satellite altitudes around 250 km, when the field of view of the detector at $\alpha \sim 90°$ is not filled by a uniform flux because it is seeing some electrons backscattered at ~ 100-km altitude where $R_\alpha < 1$.

To conclude this brief discussion about the cause of precipitation, it must be admitted that while this paper gathers together a considerable amount of experimental information about precipitation, the author remains ignorant of its cause. The tendency towards isotropy seems aesthetically attractive, although it is not clear why it should be attractive. Perhaps it is because other conceivable alternatives appear repulsive [Dessler, private communication].

Typical questions which can be required tests of a precipitation theory are listed below:

(a) Where were the individual precipitated electrons and protons yesterday, or ten seconds ago?

(b) How can the source sustain an average energy dissipation or order one hundred thousand megawatts?

(c) What causes isotropy, i.e., the "communication" between trapped and precipitated electrons of similar energies?

(d) How can high-energy ($E_e \sim 1$ MeV) trapped electrons remain essentially unaffected by the precipitation mechanism?

(e) If the energy source is the solar wind, blowing continuously, what parameter(s) of the solar wind change in such a way as to vary the precipitation intensity by a factor of one million, the energy spectra so greatly, the temporal and spatial characteristics so greatly, and so on?

(f) Why does daytime precipitation occur? And why does nighttime precipitation occur?

(g) Why is VLF associated with low-energy precipitated particles (see Part V)?

(h) Why does precipitation tend to be greatest near the outer boundary of trapping?

(i) How can precipitation be produced at near-conjugate points?

Many other test questions can be devised on the basis of data presented here and elsewhere. We suggest that at least some of these questions be a compulsory examination for any proposed theories before their publication.

QUIESCENT LOSS OF PARTICLES DRIFTING IN LONGITUDE

All the above discussion has considered only sporadic precipitation or splashes. It is well known that particles can be lost by drifting longitudinally in the real magnetic field to such low altitudes that atmospheric scattering and energy loss remove them. Thus they may not be in the local loss cone over North America, say, where B is relatively large, but they may enter the local loss cone over the Rio minimum or the Capetown anomaly where B is small.

Studies of such effects were made by Forbush, Venkatesan, and McIlwain [1962], by Laughlin et al. in Part II, by Paulikas and Freden [1963], and by Vernov, Gorchakov, Logachev, Nesterov, Pisarenko, Savenko, Chudakov, and Shavrin [1962]. The mechanism of loss is understood theoretically [Walt and MacDonald, 1962] and it makes demands on the capacity of the radiation zones at all energies. It is very important at small values of L, and produces atmospheric ionization localized near the minima in B [e.g., see Cladis and Dessler, 1961]. However, it is less important at $L > 4$ and so it is not treated here [see O'Brien, 1962].

CONCLUDING COMMENTS

We attempted to present in this paper a complete description of the phenomenology of precipitation, to the extent that is possible with currently-available research results. Much of the information was derived for the first time with the satellite Injun III, but a considerable amount came from previous measurements on the ground and with balloons, rockets, and satellites.

The various characteristics of precipitation were listed above, and one or more figures were included to illustrate particular examples and general statistical summaries. All these characteristics must be explained by prospective theories of the causes of precipitation. Furthermore, it was established that certainly at low altitudes and probably at high altitudes the precipitated electrons with energies $E_e \geq 40$ keV are aware, so to speak, of what is happening to trapped electrons, and vice versa. Thus the two categories are subject to similar influences. The flux of trapped electrons of or above a given energy increases during precipitation (as the splash-catcher model predicts) rather than decreases (as the simplified leaky-bucket model predicts). In fact not only does the intensity increase, but it increases by just the correct amount necessary to tend towards isotropy (at low altitudes).

In our opinion, a major experimental study required to advance towards an understanding of the cause of precipitation

is a detailed investigation of the limits to which this isotropy is valid. It was established with Injun III that it is valid to an accuracy of ~ 10% for electrons with energy $E_e \geq 40$ keV measured at altitudes of $\ll$ 1000 kilometers with detectors with angular resolution of some tens of degrees. All these parameters must be adjusted and the test for isotropy repeated in further experiments.

ACKNOWLEDGEMENTS

Extensive use has been made in this note of data obtained with Injun III detectors constructed by L. Frank, J. Craven, D. Stilwell, and C. D. Laughlin. Messrs. Laughlin and D. A. Gurnett were responsible for much of Injun III. We thank Dr. J. A. Van Allen and Dr. A. J. Dessler for helpful discussions about our findings, and Dr. Van Allen for his sympathetic assistance of the whole Injun III program. The Office of Naval Research, and particularly Dr. J. Fregeau, made Injun III possible, and Mr. M. Votaw was also of great assistance. The National Aeronautics and Space Administration has also supported the project, particularly with tracking and telemetry, and we thank Mr. W. Lew for his help. Telemetry was also received by the Prince Albert Radar Laboratory and the National Research Council of Canada, and we thank Drs. D. C. Rose and R. S. Rettie and Mr. D. Hansen for their assistance.

APPENDIX I: Parameters Used in This Study

When the satellite became magnetically oriented (see Part I) the major portion of the data treated here was acquired. The satellite orbital location is routinely converted into the (L, B) coordinate system of McIlwain [1961]. The parameter L labels a magnetic shell on which a trapped particle bounces in latitude and drifts in longitude. Numerically, L is such that, if the geomagnetic field was that of a perfect centered dipole, then the equatorial radial distance from the center of the earth to a given magnetic shell would be L earth radii. It has been shown that magnetic storms and the steady-state solar wind distort the geomagnetic field so much that any simple notion of L as an equatorial radial distance to a given shell in the real field must be abandoned for $L > 6$, and sometimes for lower values [O'Brien, 1963]. The parameter L derived by McIlwain [1961] from a model expansion for the geomagnetic field which best fits ground measurements is still an extremely useful idealized system, and it is used throughout this note.

Occasionally it is of interest to refer the data to ground-level observations, and for such purposes we use the concept of the invariant latitude Λ, which is derived from $L \cos^2 \Lambda = 1$, and is the "latitude" at which a given L shell intersects the surface of the earth [O'Brien, 1962]. Over

North America, Λ and the centered-dipole magnetic latitude λ differ by less than about 2°.

The parameter B is the scalar value of the local magnetic field, in gauss.

The times during January and February, 1963 at which the oriented satellite crossed the magnetic shells L = 2.0, 2.5, 3.0, 3.5, etc., were calculated, and eight-second averages of Detectors 1, 4, and 5 determined. In the usual mode, each eight-second average was derived from thirty-two transmitted measurements for each detector. All raw data were examined visually by the writer, to ensure exclusion of noisy data from the computed averages (see also discussion below).

In the design of Injun III, Detectors 4 and 5 were intended to measure precipitated particles when the satellite was magnetically oriented. Their angular orientation with respect to the payload magnetic axis was chosen to satisfy this requirement at the designed altitude of about 950 kilometers at high latitudes. The actual altitude of Injun III is sometimes so much greater than this nominal altitude that occasionally even Detector 5 measures trapped particles. In order to ensure that Detector 5 data refer only to precipitated particles, i.e., those which would have mirrored at an altitude of 100 kilometers or less, use is made of the invariant relation [see Van Allen, 1963]

$$\frac{\sin^2 \alpha}{B} = \text{constant.}$$

Two forms of this relation are of particular use here,

$$\frac{\sin^2 \alpha}{B} = \frac{\sin^2 \alpha_o}{B_o} = \frac{1}{B_m}$$

where α is the pitch angle of a particle at the location where the field strength is B gauss, so that the particle mirrors at B_m (where $\alpha = 90°$) and the subscript $_o$ refers to the equatorial plane.

Thus $\sin^2 \alpha_o = \frac{B_o}{B_m}$. Numerical values are shown in Figure 25. In the earth's magnetic field, assuming a pure dipole undistorted by the solar wind, and considering only precipitated particles tending to mirror in the atmosphere, i.e., with $B_m \sim B_{100\ km}$, the relation may be written

$$\sin^2 \alpha_{oD} = \frac{B_o}{B_{100\ km}}$$

and so $$\sin^2 \alpha_{oD} \sim \frac{1}{L^3}.$$

Thus the equatorial pitch angle defining the classical loss cone varies from about 21° at L = 2, to about 3° at L = 6.

Because the solar wind greatly distorts the geomagnetic field [Cahill and Amazeen, 1963], the use of the dipole relation above between L and B_o is invalid at large values of L, and indeed by direct measurement of trapped particles it has been

shown [O'Brien, 1963] that L loses its simple applicability at $L > 6$. This is the reason why, in the text, pitch-angle distributions at the satellite altitude have been considered rather than distributions folded back to the equatorial plane.

The deviation of the geomagnetic field arising from its eccentric, non-dipole character must be considered in defining the actual loss cone at each location of the satellite. This is particularly important in this study with Detector 5 which has a half-angle field of view of 43°. In the extremely eccentric orbit of the satellite, this detector can occasionally measure trapped particles. In these studies of precipitation, data were accepted only when the local loss-cone angle α_D was greater than 50°, thereby an allowance was made for a few degrees occasional misalignment.

Since all the data were taken over North America, $B_{100\ km}$ at a given L is relatively constant as listed in Table III. Furthermore, the nominal B_o at a given L is fixed (Table III) and since B/B_o is routinely calculated at the satellite location, we can specify that for this study

$$\left(\frac{B}{B_{100\ km}}\right) >> \sin^2 50°$$

i.e., $$\frac{B}{B_o} >> \text{constant} \times f(L) .$$

The resultant tabulation of acceptable satellite locations is shown in Table III. The minimum allowable values of B at the

TABLE III

Criteria for Detector 5 to Measure
only Precipitated Particles over North America

L (earth radii)	$B_{100\ km}$ Gauss	B_o Gauss	Minimum Allowable B/B_o at Satellite
2.0	0.50	0.039	7.6
2.5	0.54	0.0198	16
3.0	0.56	0.0116	29
3.5	0.57	0.0073	46
4.0	0.57	0.0048	70
6.0	0.58	0.00145	240

satellite might have been used as satisfactory criteria in Table III instead of B/B_o. However, through Figure 25, B/B_o can be used to give a nominal equatorial pitch angle α_o immediately.

In all this study, the equatorial magnetic field strength B_o is calculated simply from the relation [McIlwain, 1961]

$B_o = \frac{0.312}{L^3}$ gauss, where L is in units of an earth radius. Since the geomagnetic field is terminated at some ten earth radii in the sunlit hemisphere, with a terminal value of B_o of order 10^{-3} to 10^{-4} gauss [Cahill and Amazeen, 1963], this relation is clearly invalid for $L \gtrsim 10$, and the distortion of the field by the solar wind causes L to lose its simple applicability at $L > 6$ [O'Brien, 1963]. The model and the above relation will still be used here at all values of L, because they provide a convenient framework for discussion. The actual equatorial pitch angles of particles measured by Injun III at large values of L may differ significantly from those assigned in this formulation. Since the actual values cannot be calculated, we continue to use the idealized values.

APPENDIX II: Sampling of Counting Rates

In the studies of this note, only electrons were discussed, and generally only electrons with energy $E_e \geq 40$ keV, measured by Detectors 1, 4, and 5. The particle fluxes were uniquely identified as electrons (see Part I) by the electron magnetic spectrometers, and by reference to the proton spectrometers of the Applied Physics Laboratory, which showed an absence of protons in the data used here /courtesy C. Bostrom and G. Pieper/.

As discussed in Part I, the telemetry format of the satellite can be changed on command from the ground. The counting rates of the three Geiger tubes can then be sampled about four times each second, about five times, about eight times or about sixteen times a second as required. Most of the results of this note deal with samples taken four times each second, since in this mode of operation all of the twenty-two scientific instruments on board are sampled, and so a detailed analysis of the particle flux can be made. Some samples of higher-resolution of Geiger data were used in this note to establish that the synchronism of the variations in their counting rates generally persists even when they are sampled as rapidly as sixteen times each second.

Each Geiger counter is prescaled by eight before its further twelve-bit accumulator is sampled by the telemetry.

The telemetry is digital, comprising twelve binary bits for each Geiger tube, and a parity-check bit for each twelve-bit word. In these studies, the Poissonian standard deviation of a counting rate is generally small in relation to the spatial and temporal variations. For example, the million-fold scatter in intensity in the auroral zone (Figure 16) is a real and natural effect. This may be checked for any given datum point by noting that each telemetered number, when multiplied by eight, gives the total counts accumulated in the register since the previous interrogation emptied it, either one-quarter or one-sixteenth of a second before, according to the chosen telemetry mode. The prescaling register is not reset to zero upon interrogation and resetting of the following twelve-bit register.

Data used here were acquired over North America. The period of one week after separation during which the satellite was spinning and tumbling (see Part I) was used to calibrate the three Geiger counters in flight, by choosing occasions when the satellite was so oriented (for a second or so) that two or three of the detectors viewed the same flux. This occurred for all three detectors, for example, when all three axes were perpendicular to $\vec{B}$. It more commonly occurred for Detectors 1 and 4 (but not Detector 5) when the axis of one was at $\alpha \sim 70°$ and the axis of the other was at $\alpha \sim 110°$ (see Figure 13).

This early period of tumbling of the satellite was also used to derive values for R_α, the "reflection" coefficient of electrons with $E \geq 40$ keV as a function of pitch angle α (see Figure 4).

APPENDIX III: Proof That Erratic Counting Rates Are Not Merely Noisy Data

Since we are dealing with greatly-fluctuating counting rates it is absolutely essential to prove that the erratic behavior on any occasion is not due merely to noise in the telemetry or data-reduction systems, or even to erratic or noisy detectors. This can be shown in several ways as follows.

First, the satellite encoder checks the parity of each twelve-bit binary word representing the accumulated counts in each register, which word is then transmitted. The parity of each word is also transmitted with it. Then, when the S.U.I. computer translates the data, it checks the parity of each twelve-bit word against its transmitted parity. If the two disagree, the computer indicates this in the printing of the output. In these studies, we have not included data when there was more than one parity error per page of data comprising more than one thousand twelve-bit words.

Second, as was shown, there is generally but not always good correlation in the sample-to-sample counting rates of the three Geiger tubes, and also of the other detectors of low-energy electrons. But detectors of more energetic electrons and of protons show no correlated changes in the soft events studied here.

Third, these fluctuations are seen in almost every pass in auroral regions, but not in the stable inner belt or artificial radiation belt at lower L values.

In conclusion, while there is a finite probability of order 0.001 or less that a single datum point may be incorrect (noisy), there is no possibility at all that the greatly-fluctuating phenomena reported here are due to technical malfunctions.

This conclusion is bolstered by the fact that similar "erratic" behavior is seen in auroras, in balloon observations of high-latitude x-rays, and by other satellites. In fact it was simply because enormous fluctuations were detected with Injun I which had one-second temporal resolution that we designed Injun III to have temporal resolution up to a factor of sixteen times faster.

Solar x-rays can be detected by the Geigers, but such occasions can be eliminated by use of the solar aspect sensors, the photometers, and the scintillation counter (see Part I).

In much of the treatment of the data, the individual quarter-second measurements have been added over thirty-two samples by a computer. The phenomena are so variable that simple criteria dictated by the computer may either accept an occasional noisy datum point or reject a valid but greatly-variable set of points. The simple parity check does not, of course, reject a

word where two bits are in error, or four, etc. In every measurement used in this study, the raw one-quarter-second samples have been inspected by the writer. Unless several of the detectors of electrons with $E \geq 40$ keV showed synchronous variations the data were rejected. It is possible that some valid data were rejected on these subjective criteria, but it is certain that no invalid data were accepted. In particular, Detector 4 sometimes measures enhanced flux at $\alpha \sim 50°$ at $L \sim 4$ and high altitudes when the other detectors observe little change. Because there is no sufficiently-sensitive detector viewing the same direction, this effect is ignored here. It may be valid and very important, but we suggest it has to be confirmed with other detectors before it is discussed in detail. It may be caused by intermittent noisiness of the instrument but it is also generally understandable in the model formulated to summarize precipitation. As a precaution against possible error, all precipitation events were measured with Detector 5, which sees enhanced fluxes only when the other detectors do. The peak counting rates of several Geiger modules differed significantly in-flight from their calibrations pre-flight (see Part I). Since we do not know why this occurred, it was extremely important to ensure that no instrumental malfunctions in flight affected our analysis. We believe that the internal consistency of the

results (e.g., the tendency towards isotropy independent of the magnitude of the fluxes being measured), their general reasonableness (e.g., detection of auroras caused by precipitated particles at appropriate latitudes) and their consistency with earlier measurements, as well as other arguments, remove any doubt about the validity of the analyses.

It must be considered whether electron scattering in the apertures of the detectors might contaminate our results. For example, a 5% increase in the apparent flux at $\alpha \sim 90°$ might be thought to be due to scattering of part of an intense flux at $\alpha \sim 50°$, say. We conclude that such scattering effects are negligible here, first because we can see no evidence of any in Detectors 4 and 5 when Detector 1 is measuring intense fluxes of trapped electrons where there is no precipitation, and second because the magnetic spectrometer sees splashes concordant with data of Detector 1, and yet the spectrometer has very sharply-defined and narrow fields of view, with rejection by more than a factor of one thousand of electrons arriving from angles only a few degrees outside the fields of view /Laughlin, private communication/.

REFERENCES

Anderson, Kinsey A., Balloon observations of x-rays in the auroral zone I, J. Geophys. Res., 65, 551-564, 1960.

Anderson, Kinsey A. and R. De Witt, Space-time association of auroral glow and x-rays at balloon altitude, J. Geophys. Res., 68, 2669-2676, 1963.

Arnoldy, R. L., R. A. Hoffman, and J. R. Winckler, Solar cosmic rays and solar radiation observed at 5,000,000 kilometers from the earth, J. Geophys. Res., 65, 3004-3007, 1960.

Basler, R. P., Radio wave absorption in the auroral ionosphere, J. Geophys. Res., 68, 4665-4681, 1963.

Brown, R. R., K. A. Anderson, C. D. Anger, and D. S. Evans, Simultaneous electron precipitation in the northern and southern auroral zones, J. Geophys. Res., 68, 2677-2684, 1963.

Cahill, L., and P. G. Amazeen, The boundary of the geomagnetic field, J. Geophys. Res., 68, 1835-1844, 1963.

Chamberlain, J. W., Physics of the Aurora and Airglow, Academic Press, New York, 1961 (a).

Chamberlain, J. W., Theory of auroral bombardment, Astrophys. J., 134, 401-424, 1961 (b).

Cladis, J. B., and A. J. Dessler, X-rays from Van Allen belt electrons, J. Geophys. Res., 66, 343-350, 1961.

Coleman, P. J., The effects of betatron accelerations upon the intensity and energy spectrum of magnetically trapped particles, J. Geophys. Res., 66, 1351-1361, 1961.

Davis, L. R., O. E. Berg, and L. H. Meredith, Direct measurements of particle fluxes in and near auroras, Space Research, Proc. Intern. Space Sci. Symp., 1st, Nice, 1960, edited by H. K. Kallmann-Bijl, North-Holland Publishing Company, Amsterdam, 721-735, 1960.

Davis, L. R., and D. Williamson, Low-energy trapped protons, Space Research, Proc. Intern. Space Sci. Symp., 3rd, Washington, D. C., 1962, to be published, North-Holland Publishing Company, Amsterdam.

Fan, C. Y., P. Meyer, and J. A. Simpson, Trapped and cosmic radiation measurements from Explorer VI, Space Research, Proc. Intern. Space Sci. Symp., 1st, Nice, 1960, edited by H. K. Kallmann-Bijl, North-Holland Publishing Company, Amsterdam, 951-966, 1960.

Farley, T. A., and N. L. Sanders, Pitch angle distributions and mirror point densities in the outer radiation zone, J. Geophys. Res., 67, 2159-2169, 1962.

Forbush, S. E., D. Venkatesan, and C. E. McIlwain, Intensity variations in the outer Van Allen radiation belt, J. Geophys. Res., 66, 2275-2287, 1961.

Frank, L., J. Freeman, and J. A. Van Allen, Recent observations of electron fluxes in the vicinity of the earth's outer magnetosphere, Space Research, Proc. Intern. Space Sci. Symp., 4th, Warsaw, 1963, to be published, North-Holland Publishing Company, Amsterdam, 1963.

Frank, L. A., J. A. Van Allen, and E. Macagno, Charged particle observations in the earth's outer magnetosphere, J. Geophys. Res., 68, 3543-3554, 1963.

Freeman, J. W., The morphology of the electron distribution in the outer radiation zone and near the magnetospheric boundary as observed by Explorer XII, State University of Iowa Publication, SUI-63-20 (117 pages), 1963.

Ivanov-Kholodny, G. S., The part played by and the source of particles observed in the ionosphere and aurorae, Planetary Space Sci., 10, 219-232, 1963.

Laughlin, C. D., T. Fritz, and D. E. Stilwell, High-latitude geophysical studies with satellite Injun III, part II: intensities and spectra of trapped electrons, J. Geophys. Res., 1963 (in course of publication).

McDiarmid, I. B., D. C. Rose, and E. Budzinski, Direct measurement of charged particles associated with auroral zone radio absorption, Canada J. Phys., 39, 1888-1900, 1960.

McIlwain, C. E., Direct measurement of protons and electrons in visible aurorae, Space Research, Proc. Intern. Space Sci. Symp., 1st, Nice, 1960, edited by H. K. Kallmann-Bijl, North-Holland Publishing Company, Amsterdam, 715-720, 1960.

McIlwain, C. E., Coordinates for mapping the distribution of magnetically trapped particles, J. Geophys. Res., 66, 3681-3692, 1961.

McIlwain, C. E., The radiation belts, natural and artificial, Science, 1963 (in course of publication).

Neugebauer, M., and C. W. Snyder, Preliminary Results from Mariner-II solar plasma experiment, Jet Propulsion Laboratory Technical Memo. N. 33-111, 1962.

O'Brien, B. J., Lifetimes of outer-zone electrons and their precipitation into the atmosphere, J. Geophys. Res., 67, 3687-3706, 1962.

O'Brien, B. J., A large diurnal variation of the geomagnetically-trapped radiation, J. Geophys. Res., 68, 989-996, 1963.

O'Brien, B. J., and C. D. Laughlin, An extremely intense electron flux at 1000 km altitude in the auroral zone, J. Geophys. Res., 67, 2667-2672, 1962.

O'Brien, B. J., C. D. Laughlin, and D. A. Gurnett, High-latitude geophysical studies with satellite Injun III, part I: description of the satellite, J. Geophys. Res., 1963 (in course of publication).

O'Brien, B. J., and H. Taylor, High-latitude geophysical studies with satellite Injun III, part IV: auroras and their excitation, J. Geophys. Res., 1963 (in course of publication).

Paulikas, G. A., and S. C. Freden, Precipitation of energetic electrons into the atmosphere, Aerospace Corp. Publication, 1963.

Pfotzer, G., A. Emhert, H. Erbe, E. Keppler, B. Hultqvist, and J. Ortner, A contribution to the morphology of x-ray bursts in the auroral zone, J. Geophys. Res., 67, 575-585, 1962.

Rosser, W., B. J. O'Brien, J. A. Van Allen, L. A. Frank, and C. D. Laughlin, Electrons in the earth's outer radiation zone, J. Geophys. Res., 67, 4533-4542, 1962.

Van Allen, J. A., Dynamics, composition and origin of geomagnetically trapped radiation, Space Science (ed. D. P. LeGalley), 226-274, John Wiley and Sons Inc. (New York), 1963.

Van Allen, J. A., and W. C. Lin, Outer radiation belt and solar proton observations with Explorer VII during March-April 1960, J. Geophys. Res., 65, 2998-3003, 1960.

Vernov, S. N., E. V. Gorchakov, Y. I. Logachev, V. E. Nesterov, N. F. Pisarenko, I. A. Savenko, A. E. Chudakov, and P. I. Shavrin, Investigations of radiation during flights of satellites, space vehicles and rockets, J. Phys. Soc. Japan, 17, Suppl. A-II, 162-187, 1962.

Vestine, E. H., Polar auroral, geomagnetic, and ionospheric disturbances, J. Geophys. Res., 65, 360-362, 1960.

Walt, M., and W. M. MacDonald, Diffusion of electrons in the Van Allen radiation belt I. treatment of particles with mirroring points at high altitude, J. Geophys. Res., 67, 5013-5034, 1962.

Winckler, J. R., Atmospheric phenomena, energetic electrons and the geomagnetic field, Technical Report No. CR-40, University of Minnesota, 1961.

Winckler, J. R., P. D. Bhavsar, and K. A. Anderson, A study of the precipitations of energetic electrons from the geomagnetic field, J. Geophys. Res., 67, 397, 1962.

FIGURE CAPTIONS

Figure 1. Sketch illustrating the use of three directional Geiger tubes on the magnetically-oriented satellite Injun III (see also Table II).

Figure 2. Validation of the simplified splash-catcher model. The photometer measures an aurora, Detector 4 measures some of the precipitated particles at $\alpha \sim 50°$ causing the aurora, and Detector 1 shows that the flux of trapped ($\alpha \sim 90°$) electrons <u>increases</u> to approximate equality with the precipitated flux. Nominal $B/B_o \sim 230$.

Figure 3. Illustration that the flux of precipitated electrons (in A) varies more with K_p than does the omnidirectional flux (mainly of trapped electrons) in the equatorial plane (in B). Each point shows the maximum respective flux encountered on an outer-zone pass. Explorer XII data from Freeman [1963].

Figure 4. Values of the reflection coefficient R_α obtained with Injun III on six passes. The measurement shown as ▲ was made with Detectors 1 and 4 (see text).

Figure 5. Illustration of a "splash", or synchronous change in counting rates of three Geiger counters with different orientations. Temporal resolution is about 0.25 seconds. Nominal $B/B_o \sim 300$.

Figure 6. Another example of a splash, with temporal resolution four times faster than in Figure 5. The satellite travelled less than 500 meters during each sample, and the cyclotron radius of these electrons at the satellite was about 20 meters. Nominal $B/B_o \sim 700$.

Figure 7. Samples of several splashes detected by three Geiger tubes viewing trapped particles (at $\alpha \sim 90°$) and precipitated particles (at $\alpha \sim 50°$ and $\alpha \sim 0°$). Note that trapping persists between splashes, and that the precipitated flux varies by a greater proportional amount than does the trapped flux, in such a manner as to approach isotropy. Nominal $B/B_o \sim 700\text{-}500$.

Figure 8. Pitch angle distributions derived from measurements at A and B of Figure 7. For simplicity it is assumed that each detector sees particles with uniform cross section over the range of pitch angles shown as a block. They actually have conical fields of view (see Table II). Nominal $B/B_o \sim 600$.

Figure 9. Samples of splashes, showing that the flux of precipitated electrons at $\alpha \sim 0°$ tends to approach the flux of trapped electrons at $\alpha \sim 90°$. The "line of equal fluxes" is that derived from preflight calibrations of the geometric factors of the detectors, and the two lines parallel to it are twenty percent above and below it.

Figure 10. Flux increments derived from splashes of Figure 9, showing that generally the flux of "fresh" particles (derived as in Figure 8) is greater at $\alpha \sim 0°$ parallel to $\vec{B}$ than perpendicular to $\vec{B}$.

Figure 11. Similar to Figure 9, except that the flux at $\alpha \sim 50°$ is compared with that at $\alpha \sim 90°$. The tendency to isotropy is apparent once more.

Figure 12. Similar to Figure 10, except that the increment of flux or the flux of "fresh" particles at $\alpha \sim 90°$ is here compared with that at $\alpha \sim 50°$, which is generally the greater.

Figure 13. Fluxes measured by Detectors 1 and 4 when both viewed equivalent pitch angles in early non-oriented passes. The "line of equal fluxes" was again derived from preflight calibrations of the geometric factors. These data therefore substantiate the accuracy of the calibrations, and also illustrate the natural scatter in sampling equal fluxes. The scatter is much less than in Figures 11 and 12.

Figure 14. Illustration that the increment of flux or the flux of "fresh" particles is more often greater at $\alpha \sim 50°$ than at $\alpha \sim 0°$. Since both are mostly greater than that at $\alpha \sim 90°$, this illustrates that in precipitation the angular distribution tends to widen by unfolding

from $\alpha \sim 90°$, rather than by simple addition of fresh particles with maximum flux at $\alpha \sim 0°$.

Figure 15. Comparison of the latitude or L profile of precipitation for two successive passes at about the same local time. Arrows illustrate range of fluctuation of intensities at given locations, and no attempt is made to show the detailed fine structure of precipitation. This figure shows that the source must be capable of supplying precipitation over both narrow and wide ranges of latitude. Satellite altitude ~ 800 km at $L \sim 4$, and ~ 400 km at large L.

Figure 16. Samples of precipitated fluxes over North America in January 1963. Each point is an eight-second average of thirty-two measurements made at half-integral values of L. The solid line gives the average flux. This figure shows that the source must be always operative near the auroral zone, and yet vary in strength by a factor of about one million.

Figure 17. Illustration of relative constancy of precipitation over some ten seconds of time or some hundred kilometers in distance. Nominal $B/B_o \sim 1000$.

Figure 18. Illustration of large variations in precipitation. Compare with Figure 17, which shows data taken about two minutes later at a high latitude. The two figures

show that the source must be capable of sustaining precipitation both extensive and restricted in latitude and/or time. Nominal $B/B_o \sim 290$.

Figure 19. Widespread precipitation observed on a northbound and the following southbound pass over North America, when the satellite took about seven minutes between successive crossings of the $L = 7.5$ shell. This shows that the source must be able to sustain intense precipitation uniformly over some 75° or about 4000 kilometers of longitude. Nominal $B/B_o \sim 700\text{-}3500$.

Figure 20. Widespread precipitation observed on a northbound and the following southbound pass over North America. This shows that the precipitation varied erratically either with local time or during some ten minutes of real time. Compare with Figure 19. Nominal $B/B_o \sim 250\text{-}3000$.

Figure 21. Same data as in Figure 20 replotted to contrast the northbound and southbound latitude profiles.

Figure 22. Intensity of precipitation in the range $6 \leq L \leq 8$ versus local time. This shows that the source must be capable of supplying large and small fluxes during the day and during the night. During the first three months in orbit the satellite made no passes over North America between local hours of 1600 and 2100.

Figure 23. Similar to Figure 22 but for the range $8.5 \leq L \leq 11$. Similar conclusions can be drawn about the source. The flux of trapped electrons over this range shows a very marked diurnal variation [see O'Brien, 1963].

Figure 24. Flux of electrons precipitated at $L = 6.0$ and $L = 6.5$ during January 1963. This shows that precipitation is generally more intense during magnetic storms as measured by the planetary magnetic disturbance index K_p. When measurements were made at both values of L on a given pass they are shown joined by a line.

Figure 25. Dependence on B_m/B_o of the equatorial pitch angle α_o at an equatorial field strength of B_o gauss of a particle which will mirror at a field strength B_m. The curve is drawn on the assumption of conservation of the magnetic moment of the spiralling electron. If the geomagnetic field were of a centered undistorted dipole form, $B_m/B_o \sim L^3$. In reality, this is invalid for $L \gtrsim 6$.

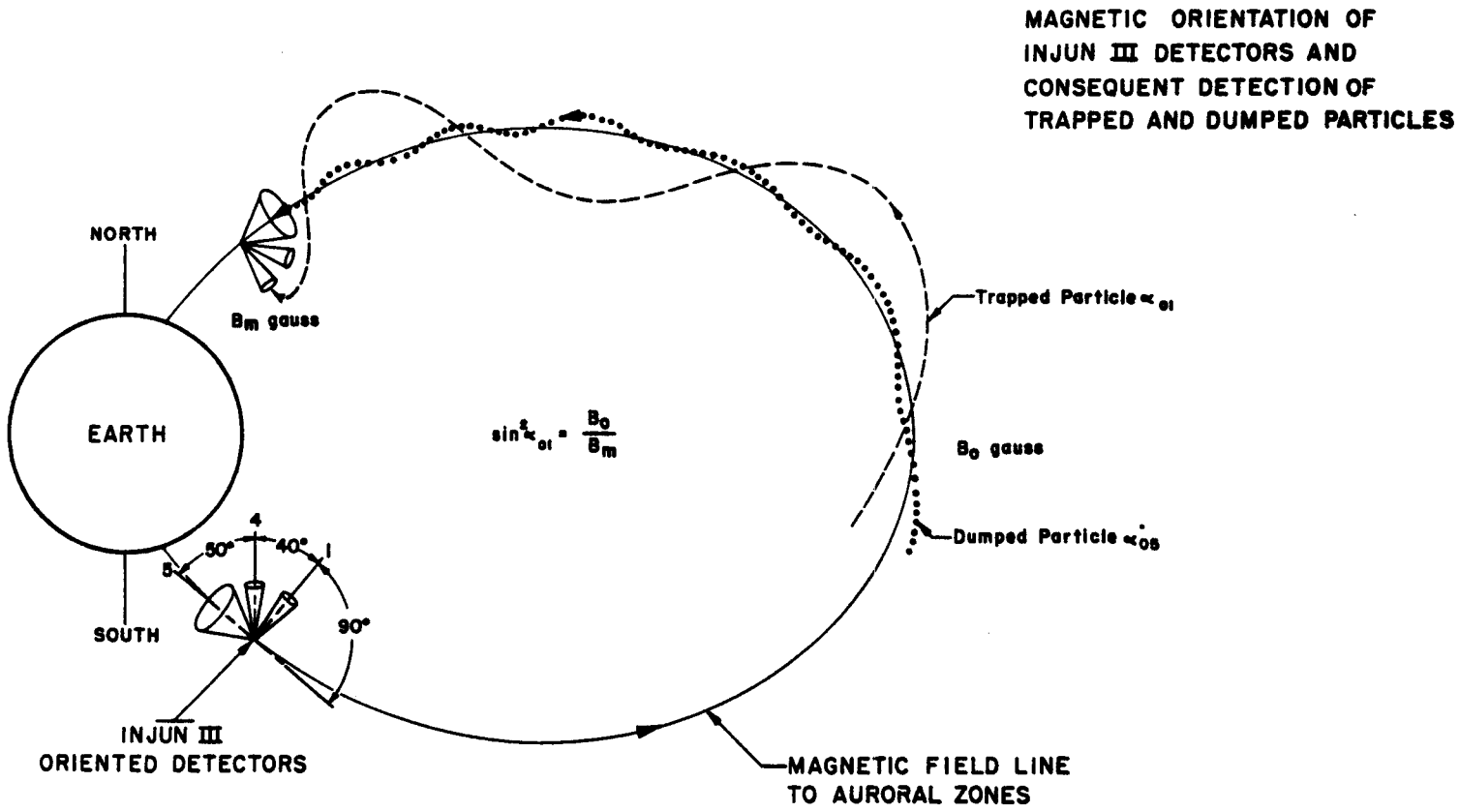
MAGNETIC ORIENTATION OF
INJUN III DETECTORS AND
CONSEQUENT DETECTION OF
TRAPPED AND DUMPED PARTICLES
NORTH
EARTH
SOUTH
Bm gauss
$\sin^2\alpha_{ot} = \frac{B_o}{B_m}$
Trapped Particle α_{ot}
B_o gauss
Dumped Particle α_{os}
4
50°
40°
1
5
90°
INJUN III
ORIENTED DETECTORS
MAGNETIC FIELD LINE
TO AURORAL ZONES

Figure 1

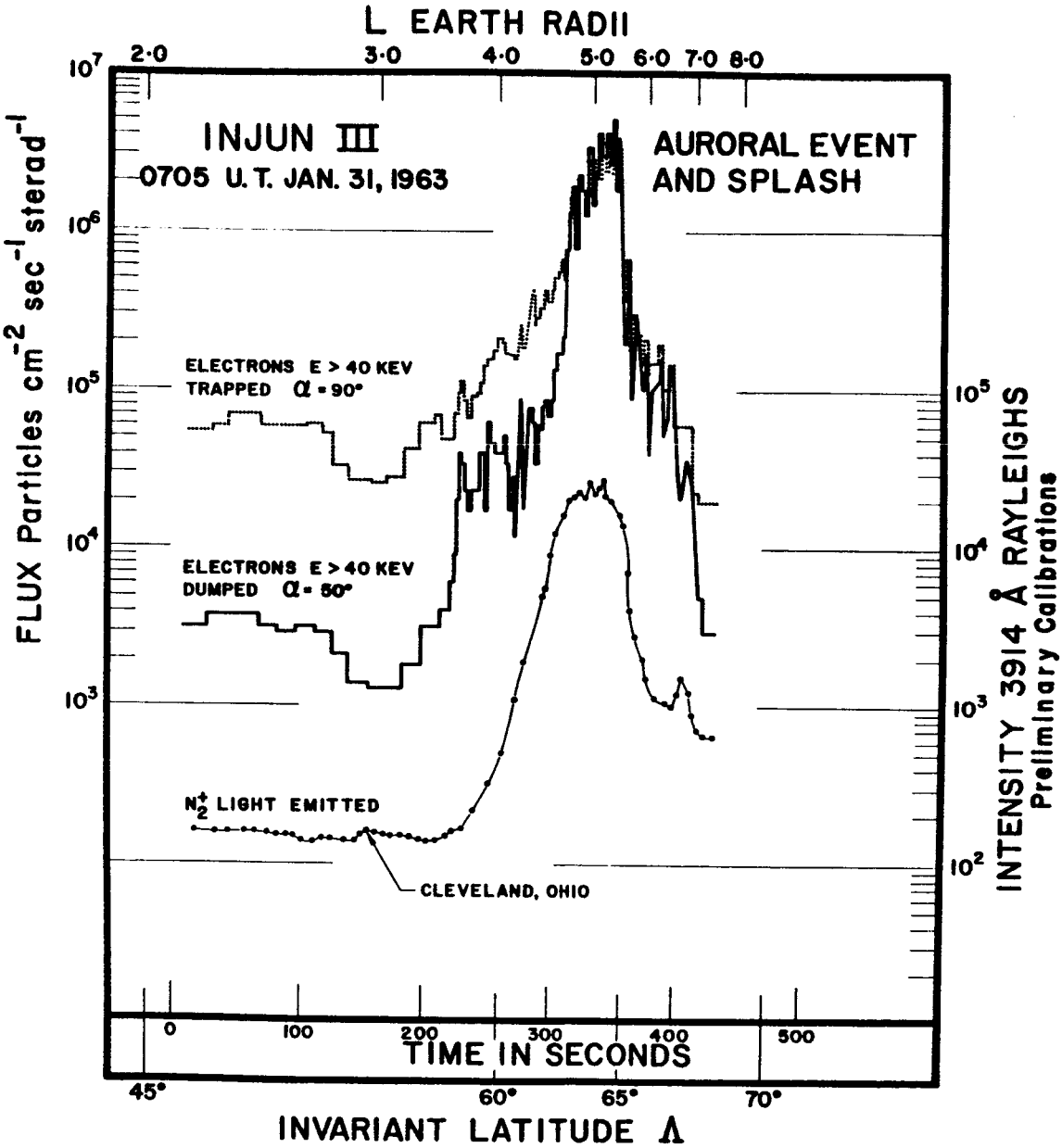
L EARTH RADII
2·0
3·0
4·0
5·0
6·0
7·0
8·0
INJUN III
0705 U.T. JAN. 31, 1963
AURORAL EVENT
AND SPLASH
ELECTRONS E > 40 KEV
TRAPPED α = 90°
ELECTRONS E > 40 KEV
DUMPED α = 50°
N2+ LIGHT EMITTED
CLEVELAND, OHIO
FLUX Particles cm-2 sec-1 sterad-1
INTENSITY 3914 Å RAYLEIGHS
Preliminary Calibrations
TIME IN SECONDS
INVARIANT LATITUDE Λ

Figure 2

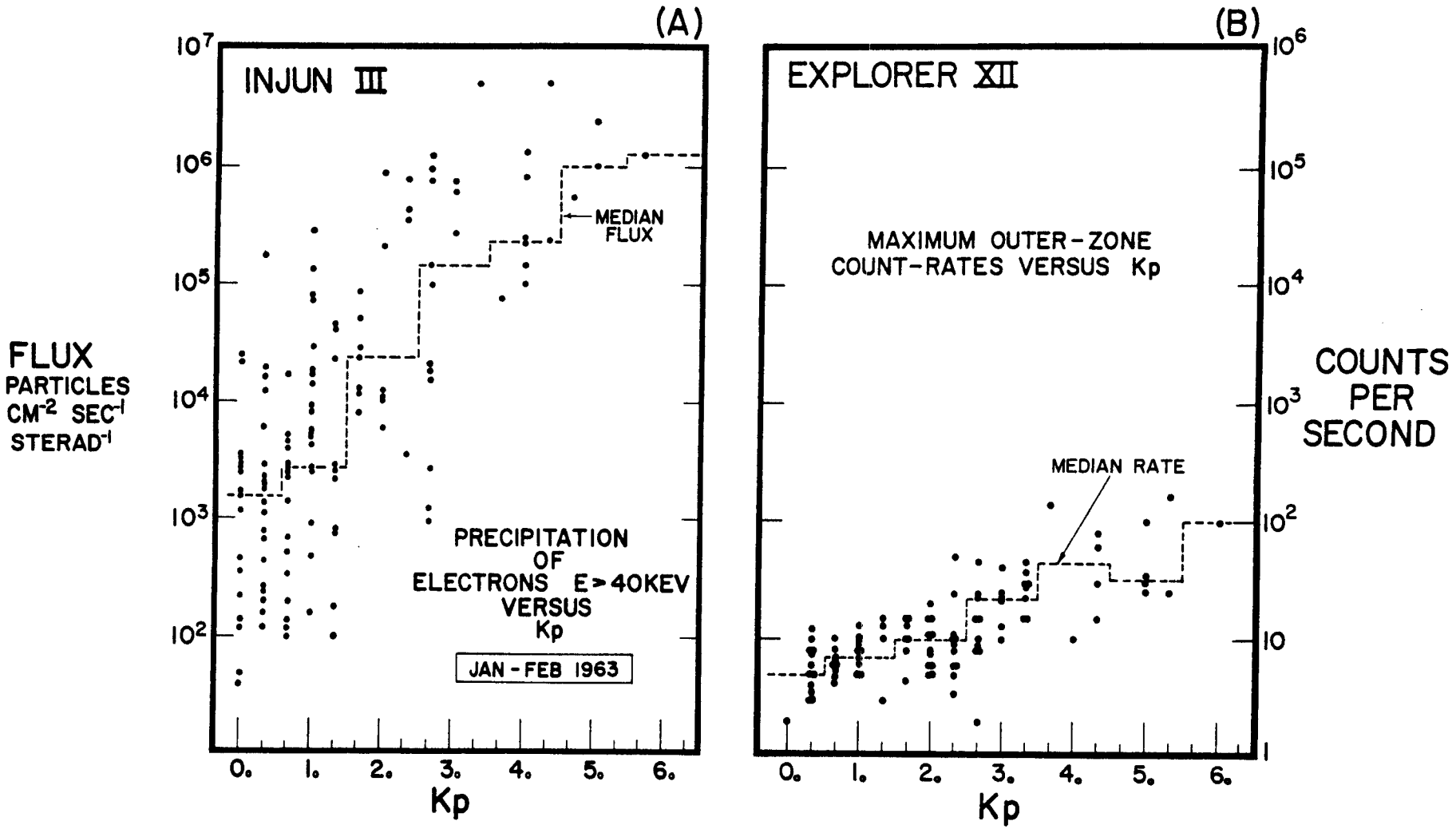
(A)
INJUN III
MEDIAN FLUX
PRECIPITATION OF ELECTRONS E>40KEV VERSUS Kp
JAN - FEB 1963
FLUX PARTICLES CM-2 SEC-1 STERAD-1
Kp
(B)
EXPLORER XII
MAXIMUM OUTER-ZONE COUNT-RATES VERSUS Kp
MEDIAN RATE
COUNTS PER SECOND
Kp

Figure 3

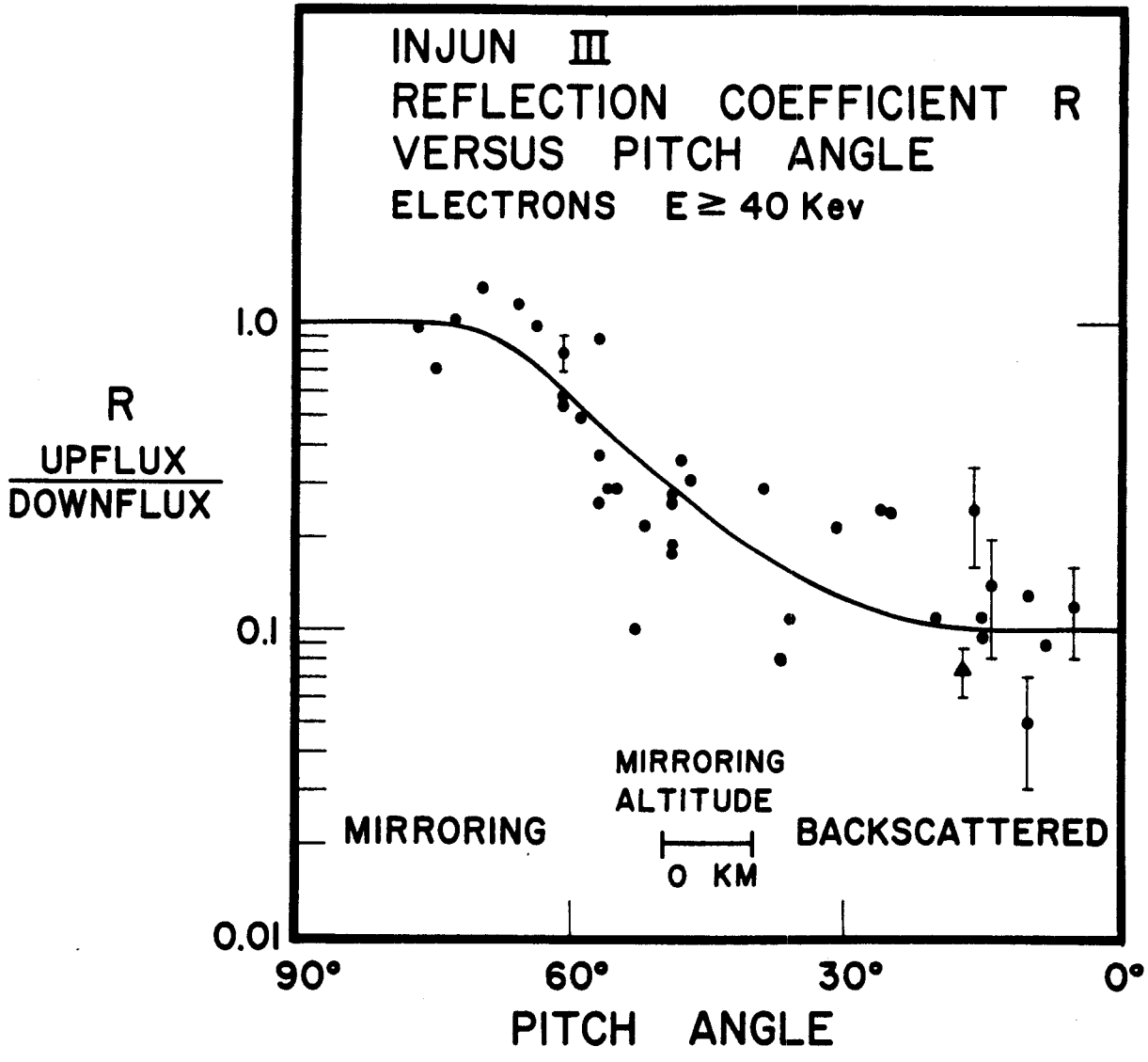
INJUN III
REFLECTION COEFFICIENT R
VERSUS PITCH ANGLE
ELECTRONS E ≥ 40 Kev
R
UPFLUX
DOWNFLUX
1.0
0.1
0.01
MIRRORING
MIRRORING
ALTITUDE
0 KM
BACKSCATTERED
90°
60°
30°
0°
PITCH ANGLE

Figure 4

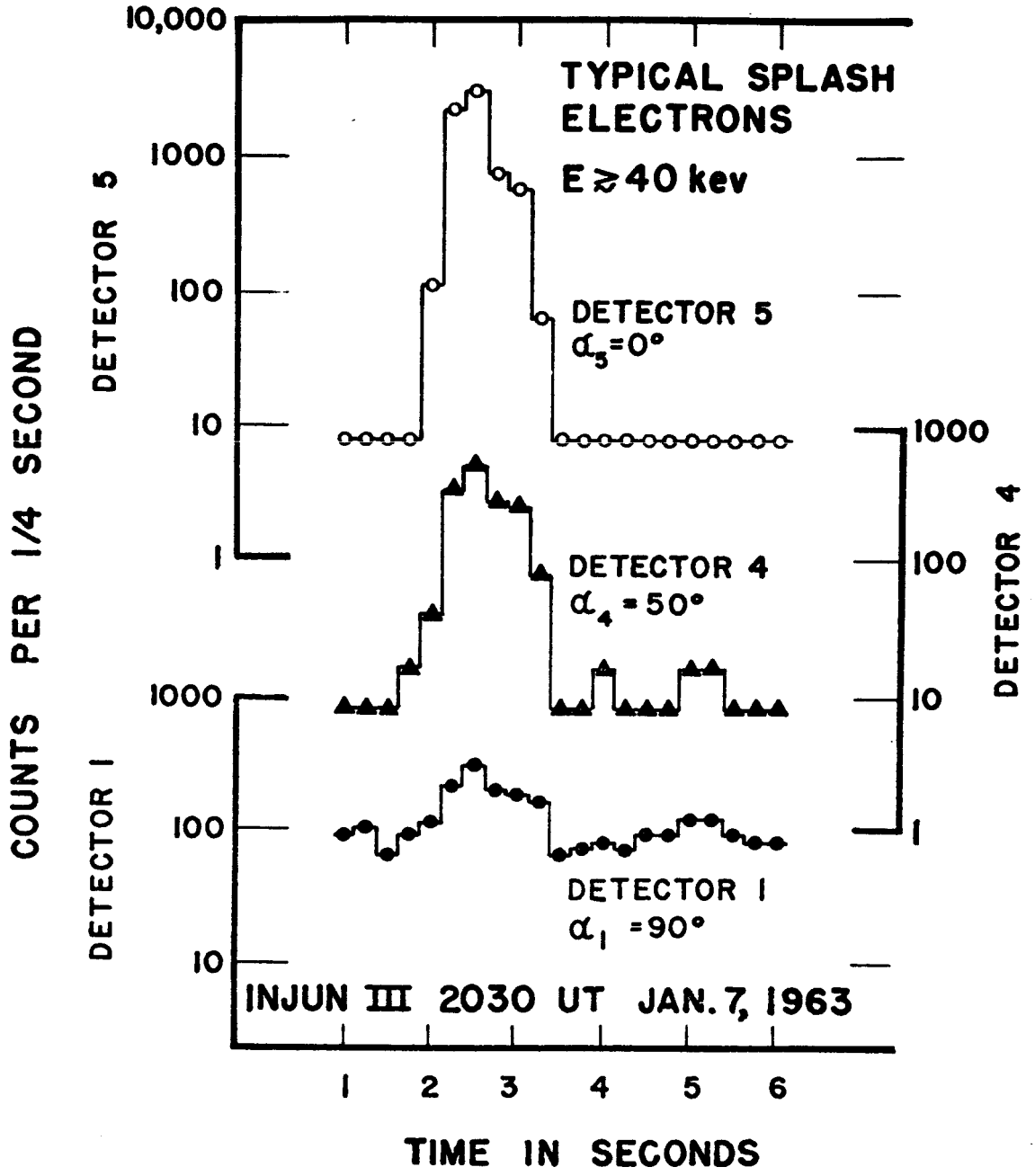
TYPICAL SPLASH ELECTRONS
E ≳ 40 kev
DETECTOR 5
$\alpha_5 = 0°$
DETECTOR 4
$\alpha_4 = 50°$
DETECTOR 1
$\alpha_1 = 90°$
INJUN III 2030 UT JAN. 7, 1963
COUNTS PER 1/4 SECOND
DETECTOR 5
DETECTOR 1
DETECTOR 4
10,000
1000
100
10
1
1000
100
10
1
1000
100
10
1 2 3 4 5 6
TIME IN SECONDS

Figure 5

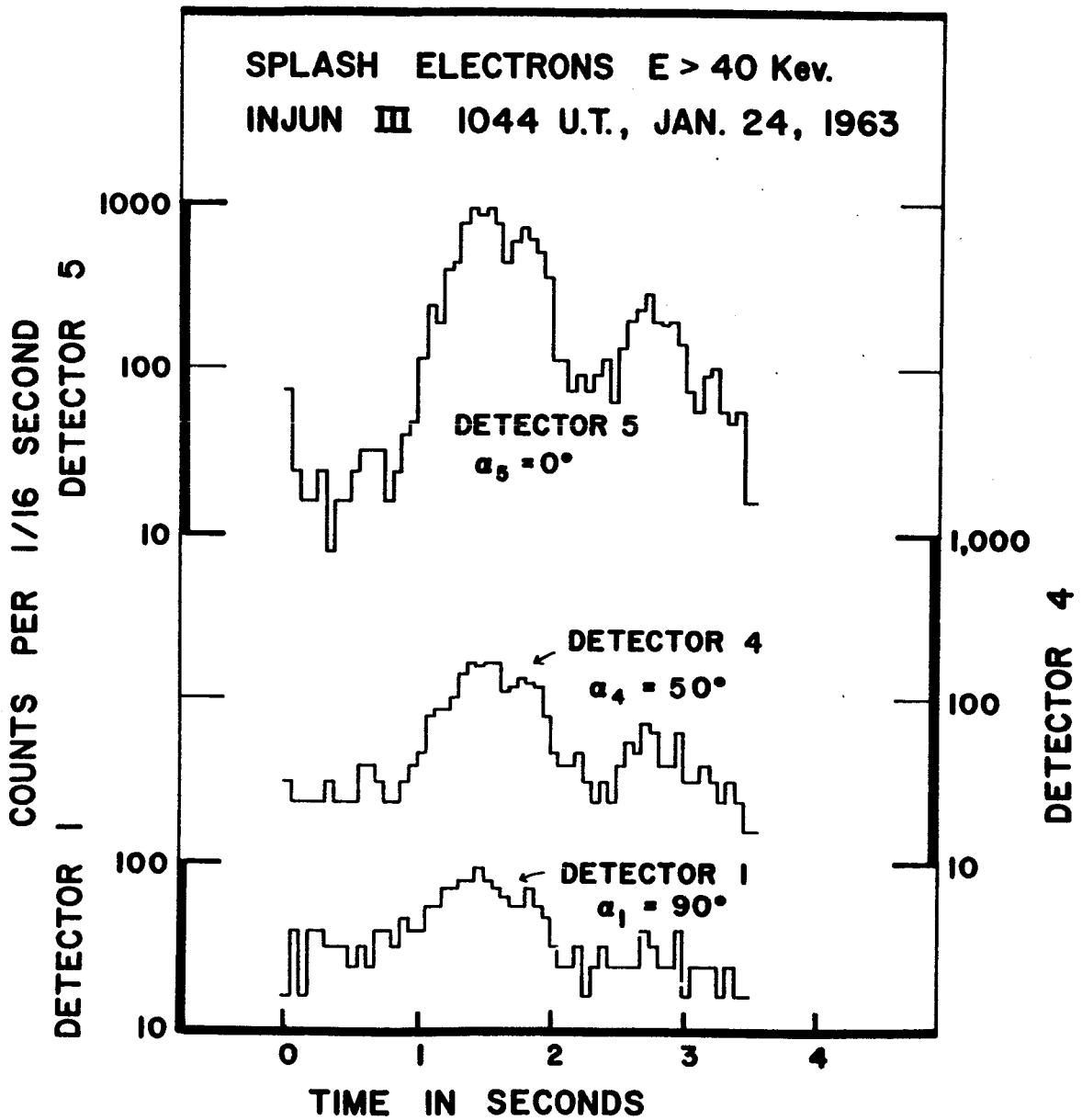
SPLASH ELECTRONS E > 40 Kev.
INJUN III 1044 U.T., JAN. 24, 1963
COUNTS PER 1/16 SECOND
DETECTOR 5
DETECTOR 4
DETECTOR 1
1000
100
10
1,000
100
10
DETECTOR 5
$\alpha_5 = 0°$
DETECTOR 4
$\alpha_4 = 50°$
DETECTOR 1
$\alpha_1 = 90°$
0
1
2
3
4
TIME IN SECONDS

Figure 6

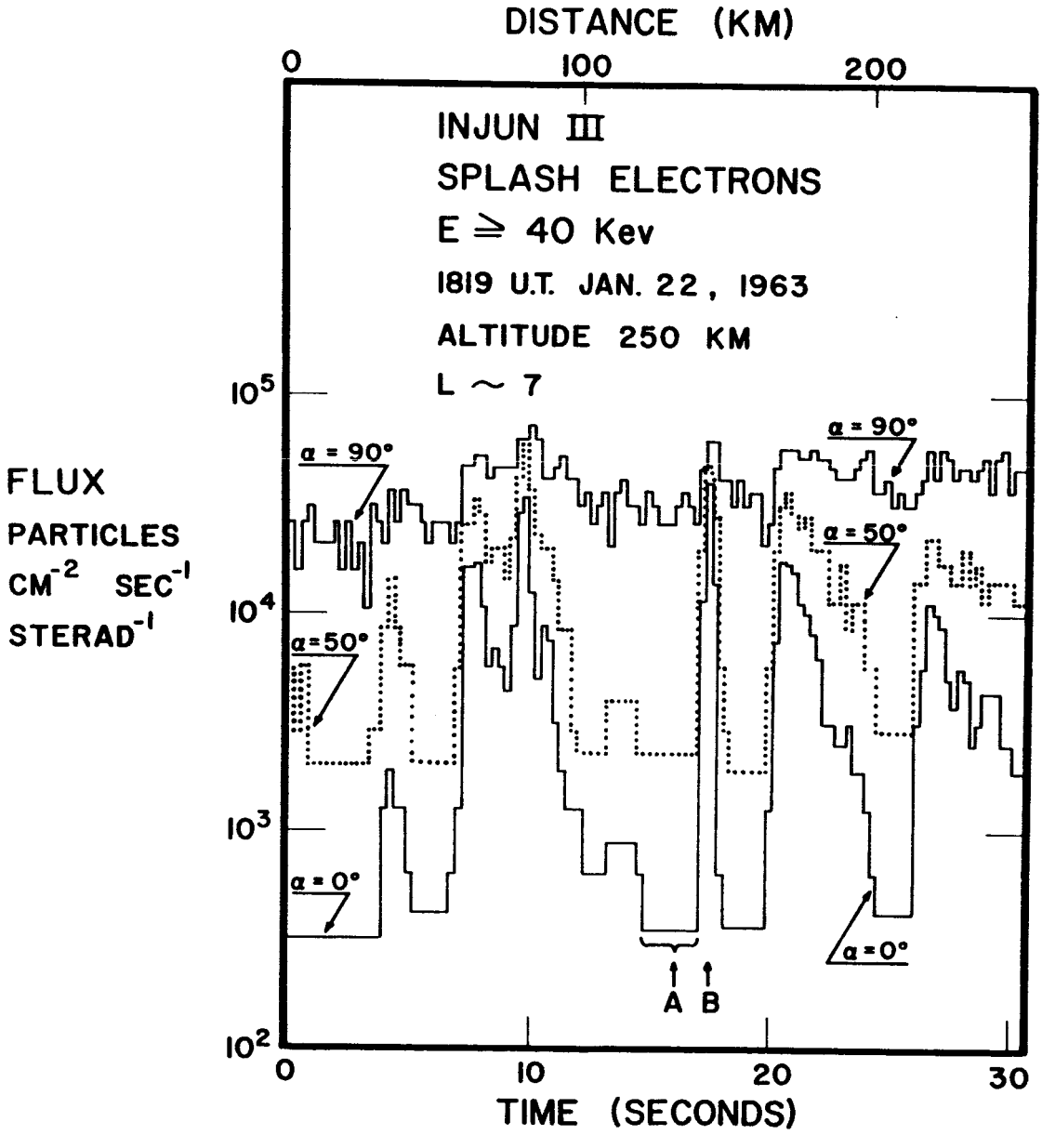
DISTANCE (KM)
0
100
200
INJUN III
SPLASH ELECTRONS
E ≧ 40 Kev
1819 U.T. JAN. 22, 1963
ALTITUDE 250 KM
L ~ 7
FLUX
PARTICLES
CM-2 SEC-1
STERAD-1
10^5
10^4
10^3
10^2
α = 90°
α = 50°
α = 0°
A
B
0
10
20
30
TIME (SECONDS)

Figure 7

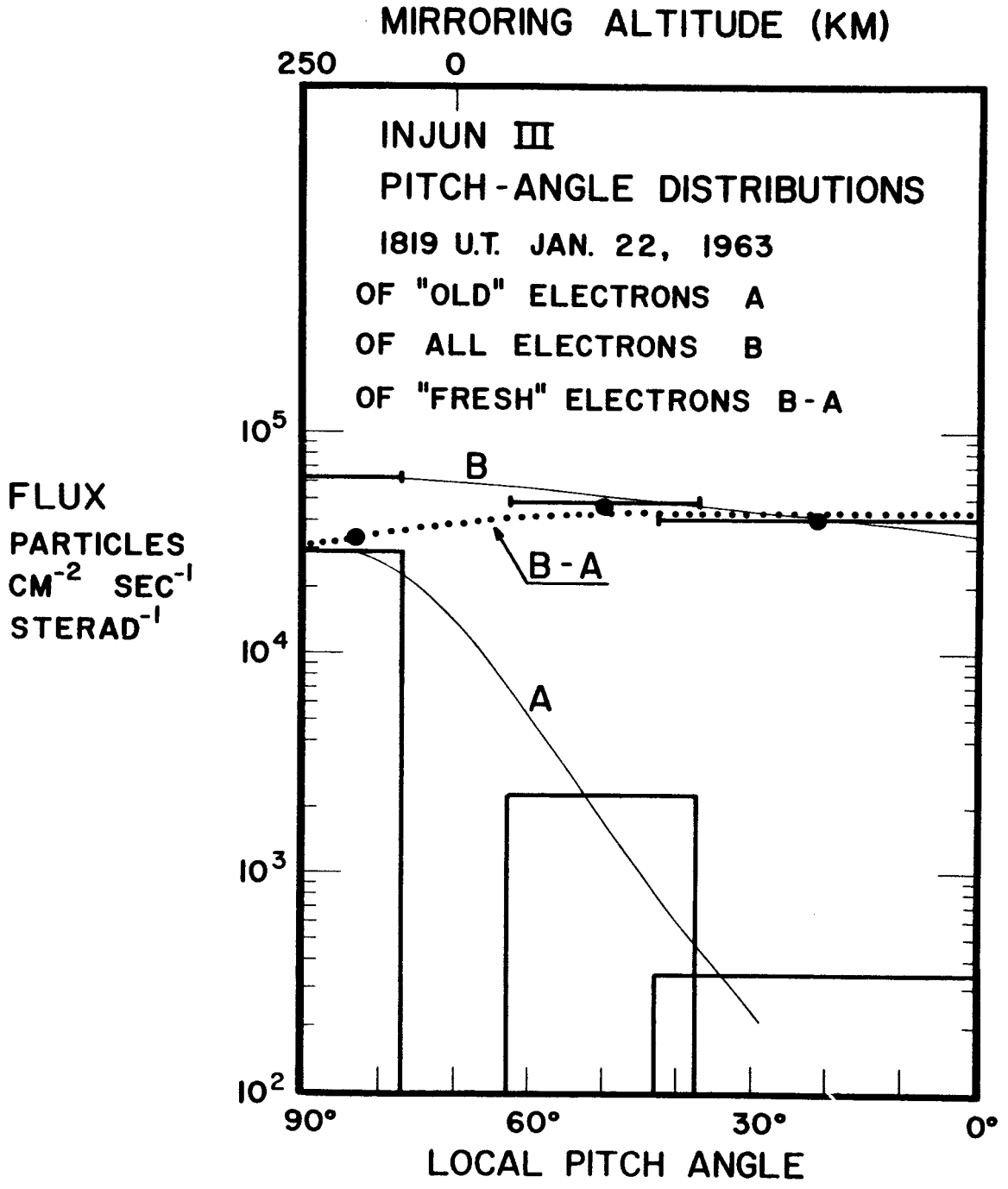
MIRRORING ALTITUDE (KM)
250
0
INJUN III
PITCH-ANGLE DISTRIBUTIONS
1819 U.T. JAN. 22, 1963
OF "OLD" ELECTRONS A
OF ALL ELECTRONS B
OF "FRESH" ELECTRONS B-A
FLUX
PARTICLES
CM-2 SEC-1
STERAD-1
10^5
10^4
10^3
10^2
B
B-A
A
90°
60°
30°
0°
LOCAL PITCH ANGLE

Figure 8

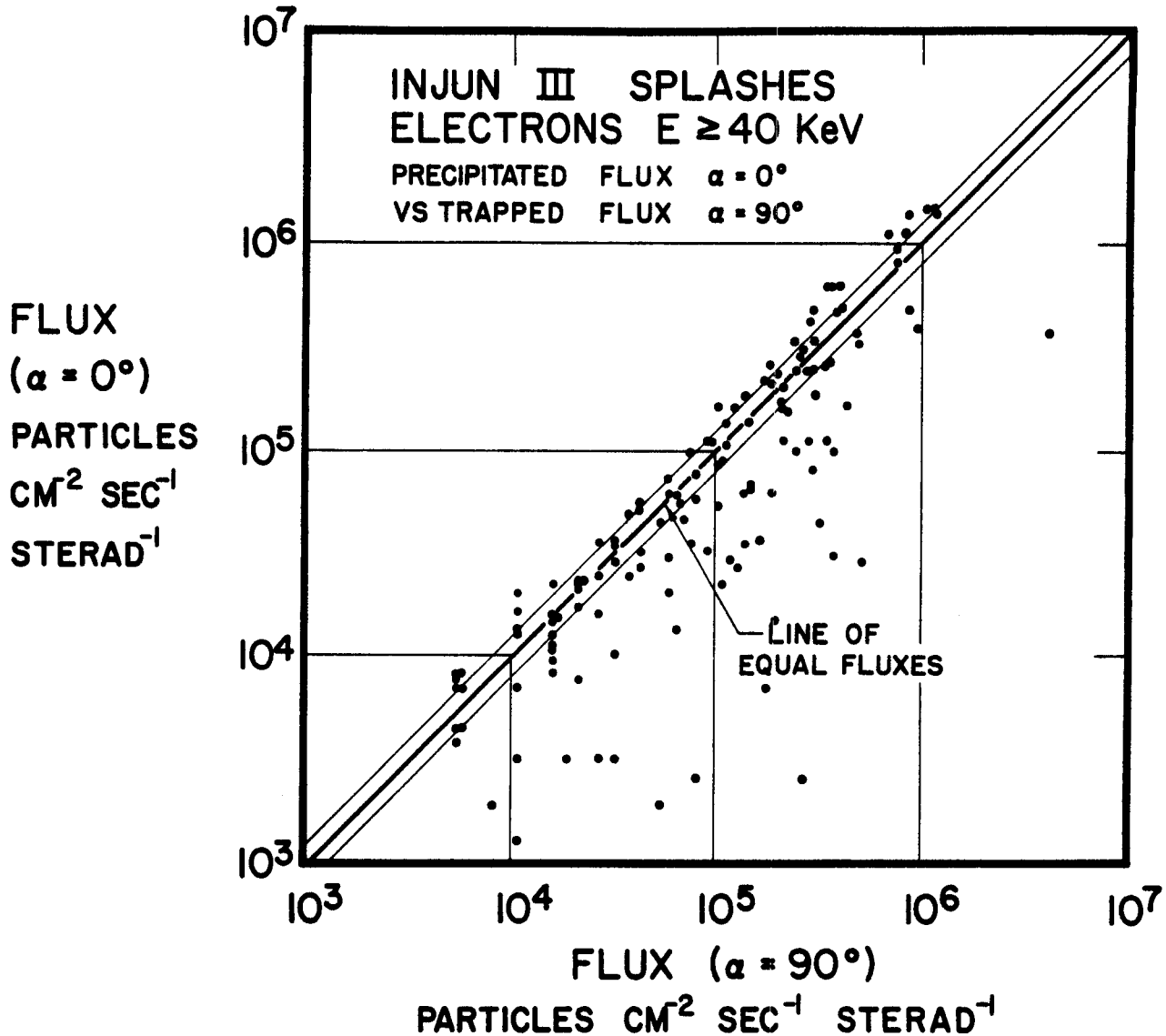
INJUN III SPLASHES
ELECTRONS E ≥ 40 KeV
PRECIPITATED FLUX α = 0°
VS TRAPPED FLUX α = 90°
LINE OF EQUAL FLUXES
FLUX (α = 0°) PARTICLES CM⁻² SEC⁻¹ STERAD⁻¹
FLUX (α = 90°) PARTICLES CM⁻² SEC⁻¹ STERAD⁻¹
10³
10⁴
10⁵
10⁶
10⁷

Figure 9

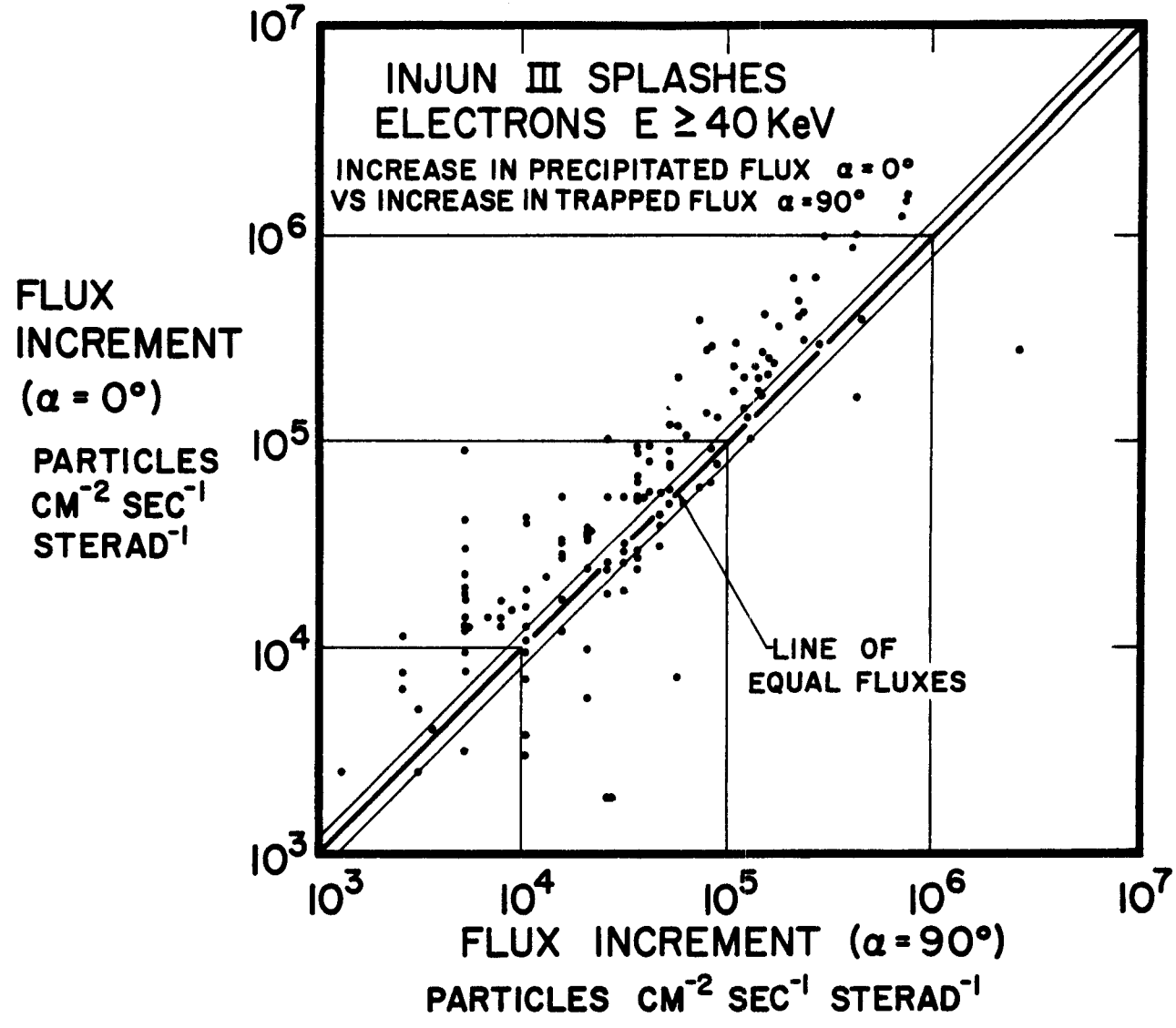
INJUN III SPLASHES
ELECTRONS E ≥ 40 KeV
INCREASE IN PRECIPITATED FLUX α = 0°
VS INCREASE IN TRAPPED FLUX α = 90°
FLUX INCREMENT (α = 0°)
PARTICLES CM⁻² SEC⁻¹ STERAD⁻¹
LINE OF EQUAL FLUXES
10³
10⁴
10⁵
10⁶
10⁷
FLUX INCREMENT (α = 90°)
PARTICLES CM⁻² SEC⁻¹ STERAD⁻¹

Figure 10

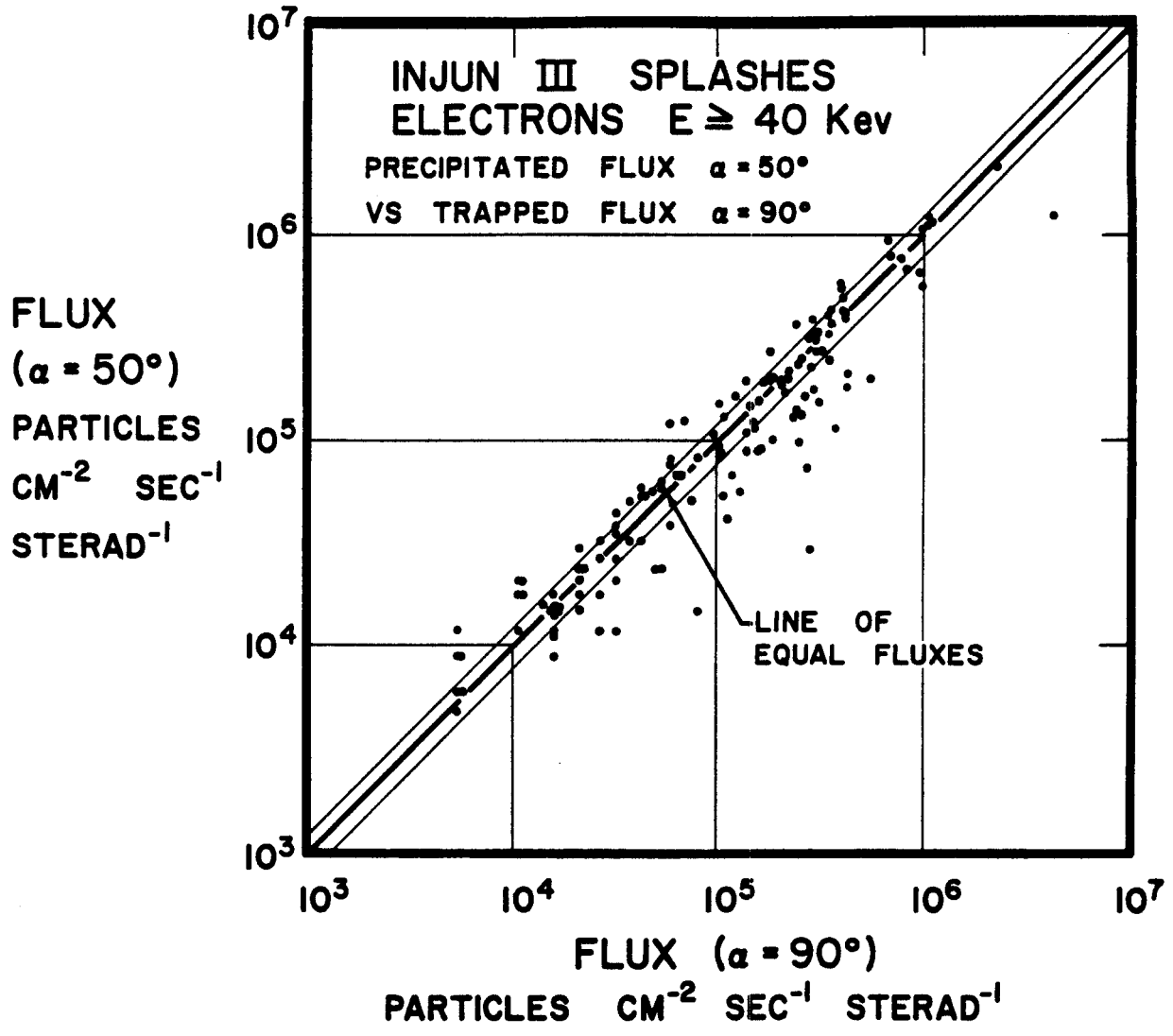
INJUN III SPLASHES
ELECTRONS E ≥ 40 Kev
PRECIPITATED FLUX α = 50°
VS TRAPPED FLUX α = 90°
LINE OF EQUAL FLUXES
FLUX (α = 50°) PARTICLES CM-2 SEC-1 STERAD-1
FLUX (α = 90°) PARTICLES CM-2 SEC-1 STERAD-1
10^7
10^6
10^5
10^4
10^3

Figure 11

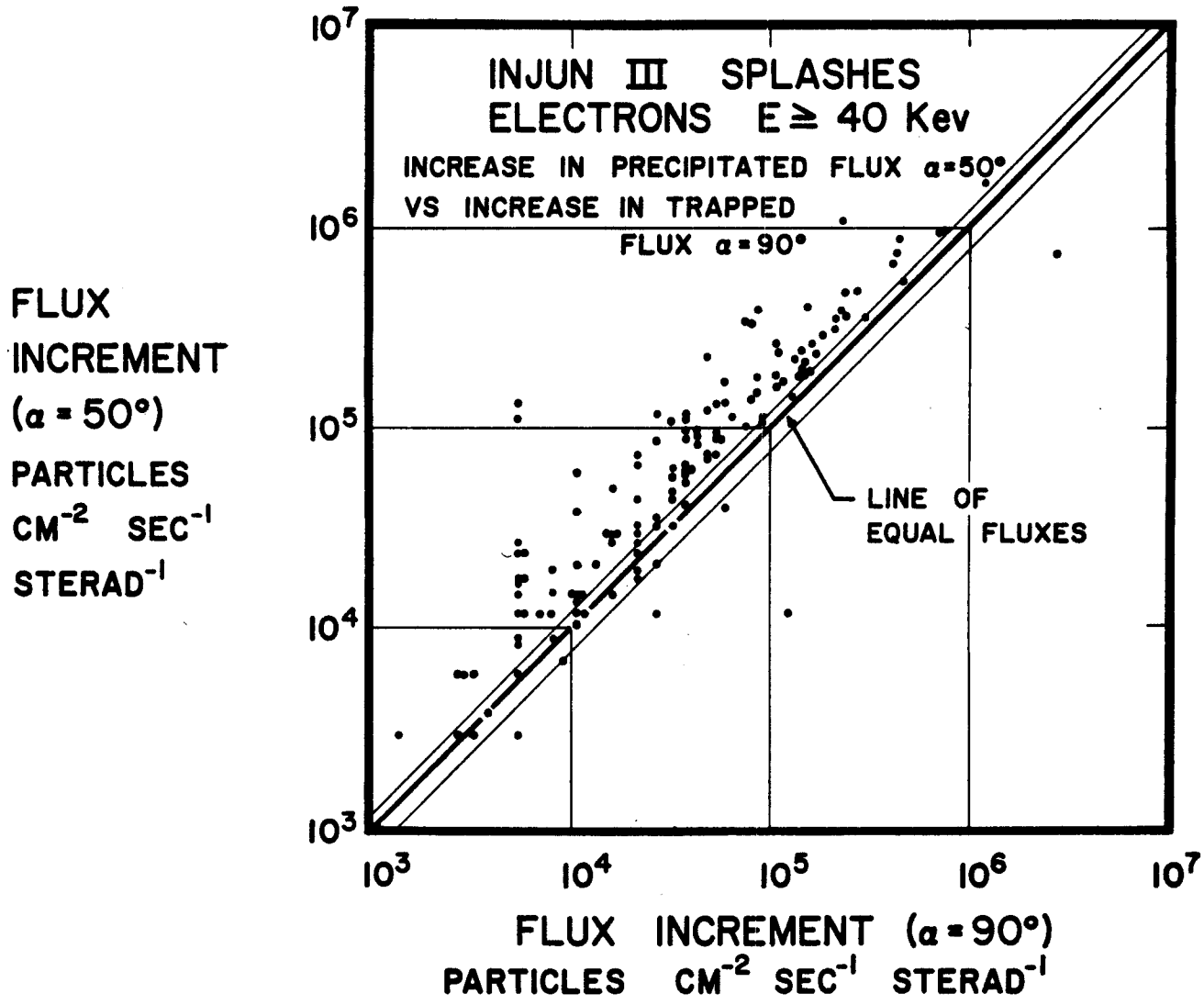
INJUN III SPLASHES
ELECTRONS E ≥ 40 Kev
INCREASE IN PRECIPITATED FLUX α=50°
VS INCREASE IN TRAPPED
FLUX α=90°
LINE OF
EQUAL FLUXES
FLUX
INCREMENT
(α = 50°)
PARTICLES
CM-2 SEC-1
STERAD-1
10^7
10^6
10^5
10^4
10^3
10^3
10^4
10^5
10^6
10^7
FLUX INCREMENT (α = 90°)
PARTICLES CM-2 SEC-1 STERAD-1

Figure 12

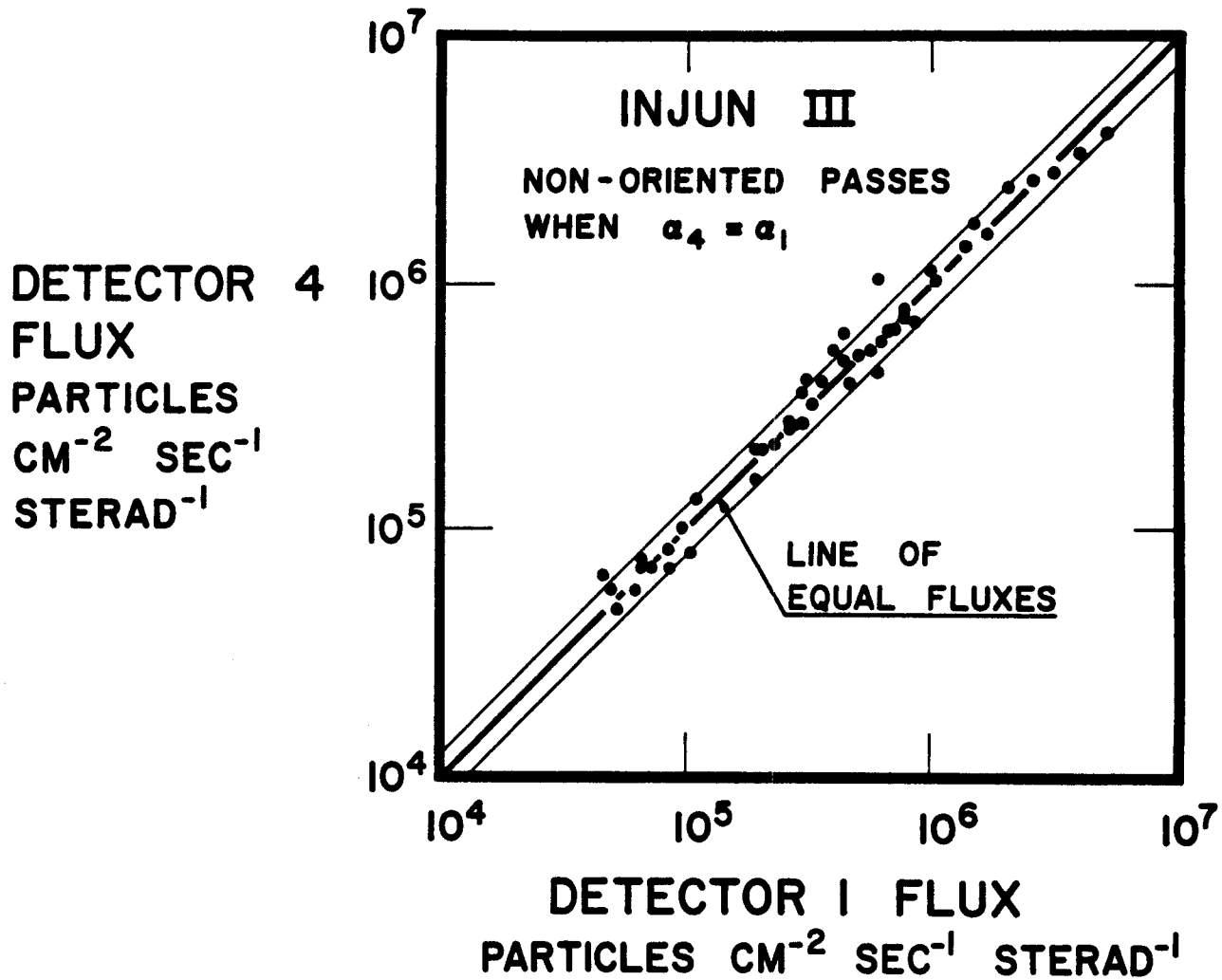
INJUN III
NON-ORIENTED PASSES
WHEN $\alpha_4 = \alpha_1$
LINE OF
EQUAL FLUXES
10^7
10^6
10^5
10^4
10^4
10^5
10^6
10^7
DETECTOR 4
FLUX
PARTICLES
CM^{-2} SEC^{-1}
$STERAD^{-1}$
DETECTOR 1 FLUX
PARTICLES CM^{-2} SEC^{-1} $STERAD^{-1}$

Figure 13

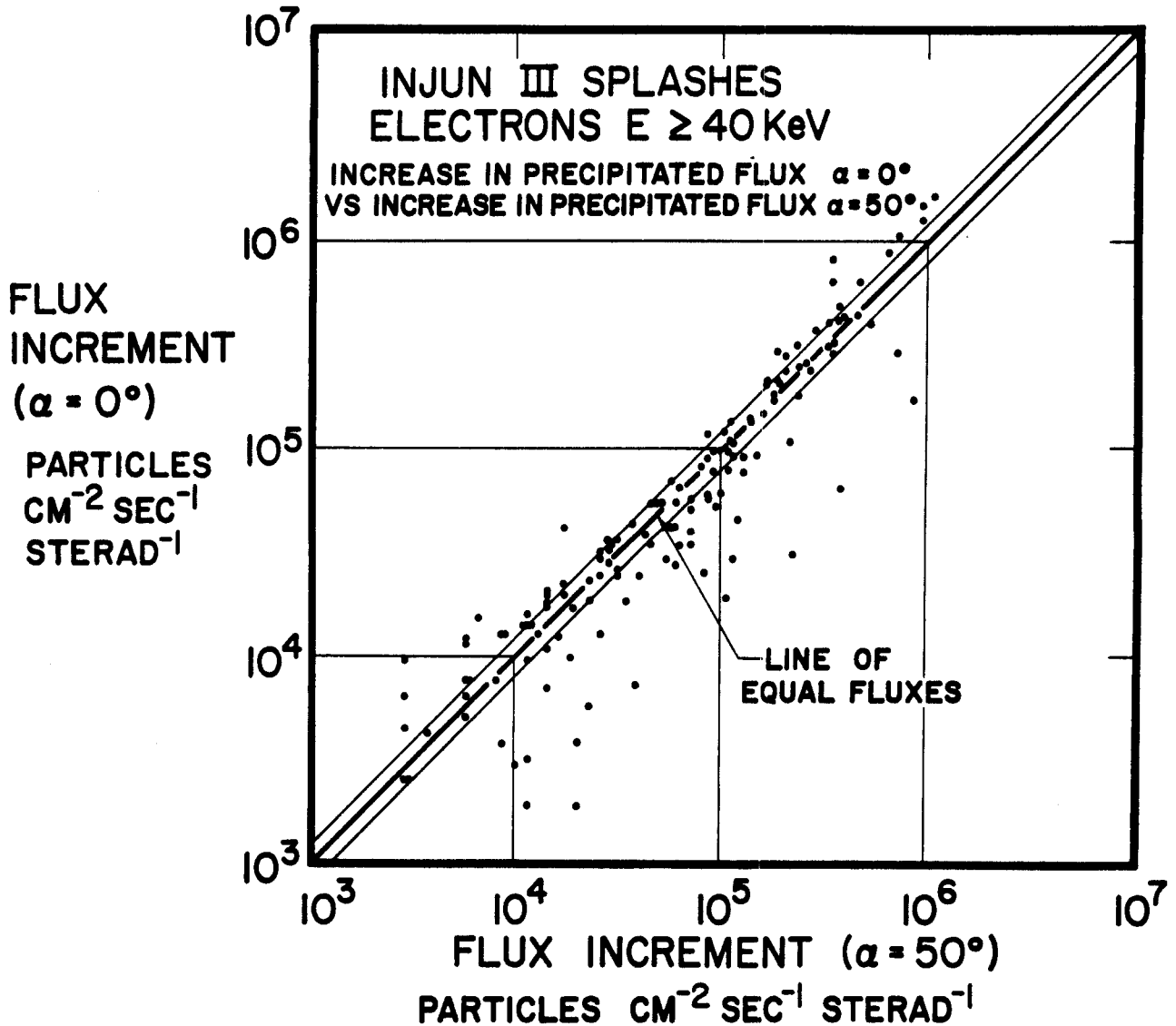
INJUN III SPLASHES
ELECTRONS E ≥ 40 KeV
INCREASE IN PRECIPITATED FLUX α = 0°
VS INCREASE IN PRECIPITATED FLUX α = 50°
FLUX INCREMENT (α = 0°)
PARTICLES CM⁻² SEC⁻¹ STERAD⁻¹
LINE OF EQUAL FLUXES
FLUX INCREMENT (α = 50°)
PARTICLES CM⁻² SEC⁻¹ STERAD⁻¹
10³
10⁴
10⁵
10⁶
10⁷

Figure 14

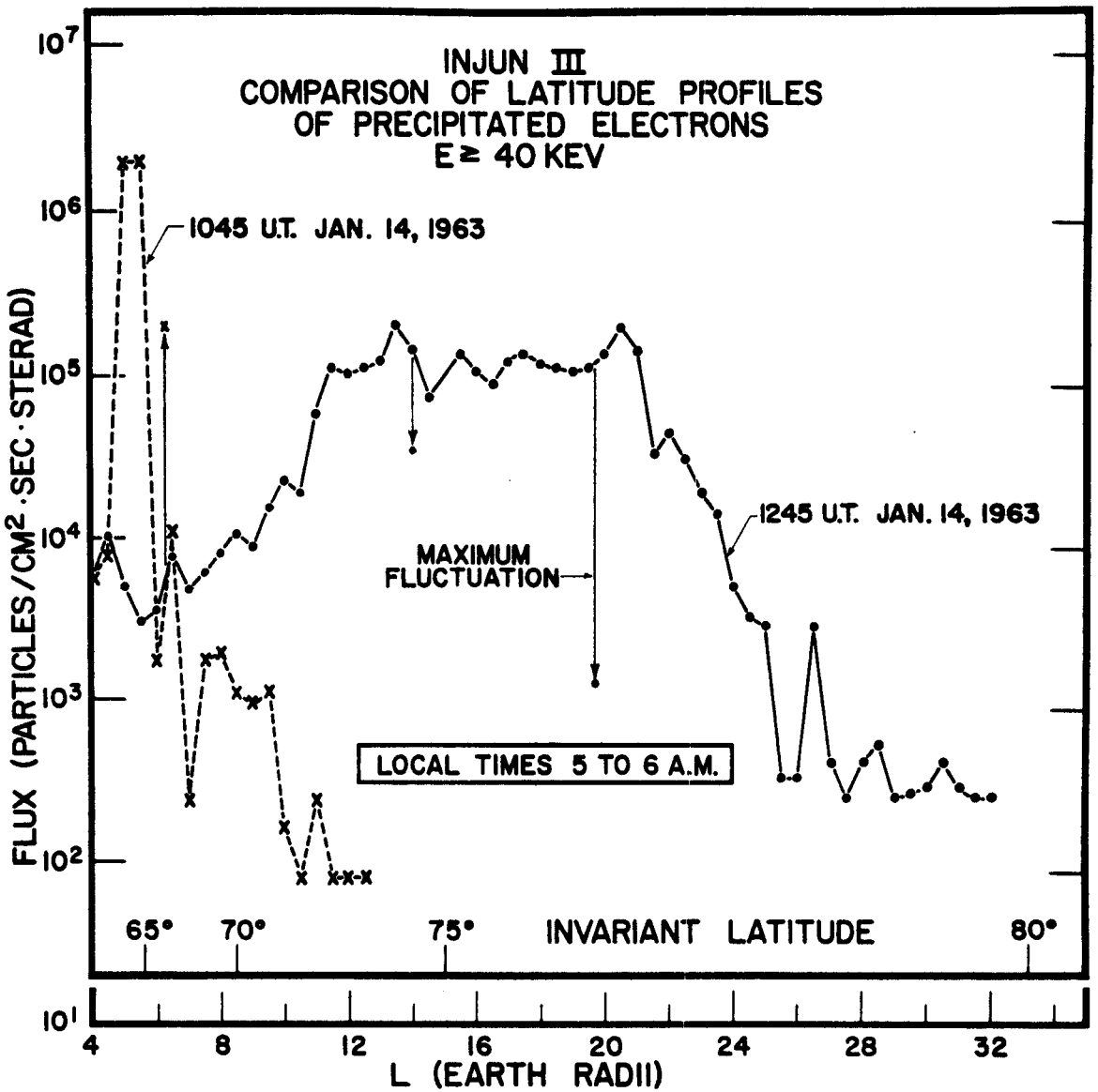
INJUN III
COMPARISON OF LATITUDE PROFILES
OF PRECIPITATED ELECTRONS
E ≥ 40 KEV
1045 U.T. JAN. 14, 1963
1245 U.T. JAN. 14, 1963
MAXIMUM
FLUCTUATION
LOCAL TIMES 5 TO 6 A.M.
FLUX (PARTICLES/CM² · SEC · STERAD)
INVARIANT LATITUDE
L (EARTH RADII)
10⁷
10⁶
10⁵
10⁴
10³
10²
10¹
65°
70°
75°
80°
4
8
12
16
20
24
28
32

Figure 15

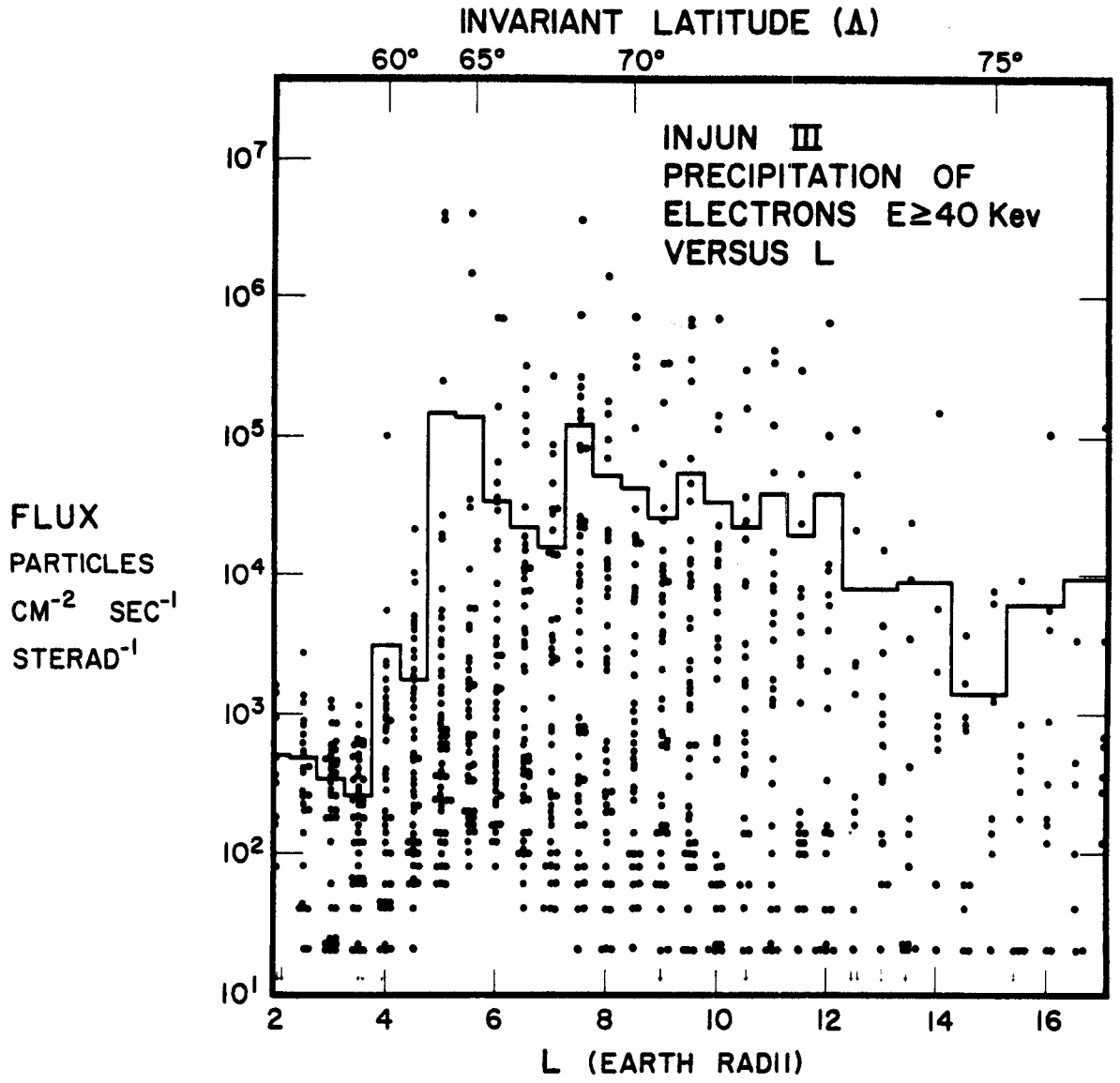
INVARIANT LATITUDE (Λ)
60°
65°
70°
75°
INJUN III
PRECIPITATION OF
ELECTRONS E≥40 Kev
VERSUS L
FLUX
PARTICLES
CM-2 SEC-1
STERAD-1
10^7
10^6
10^5
10^4
10^3
10^2
10^1
2
4
6
8
10
12
14
16
L (EARTH RADII)

Figure 16

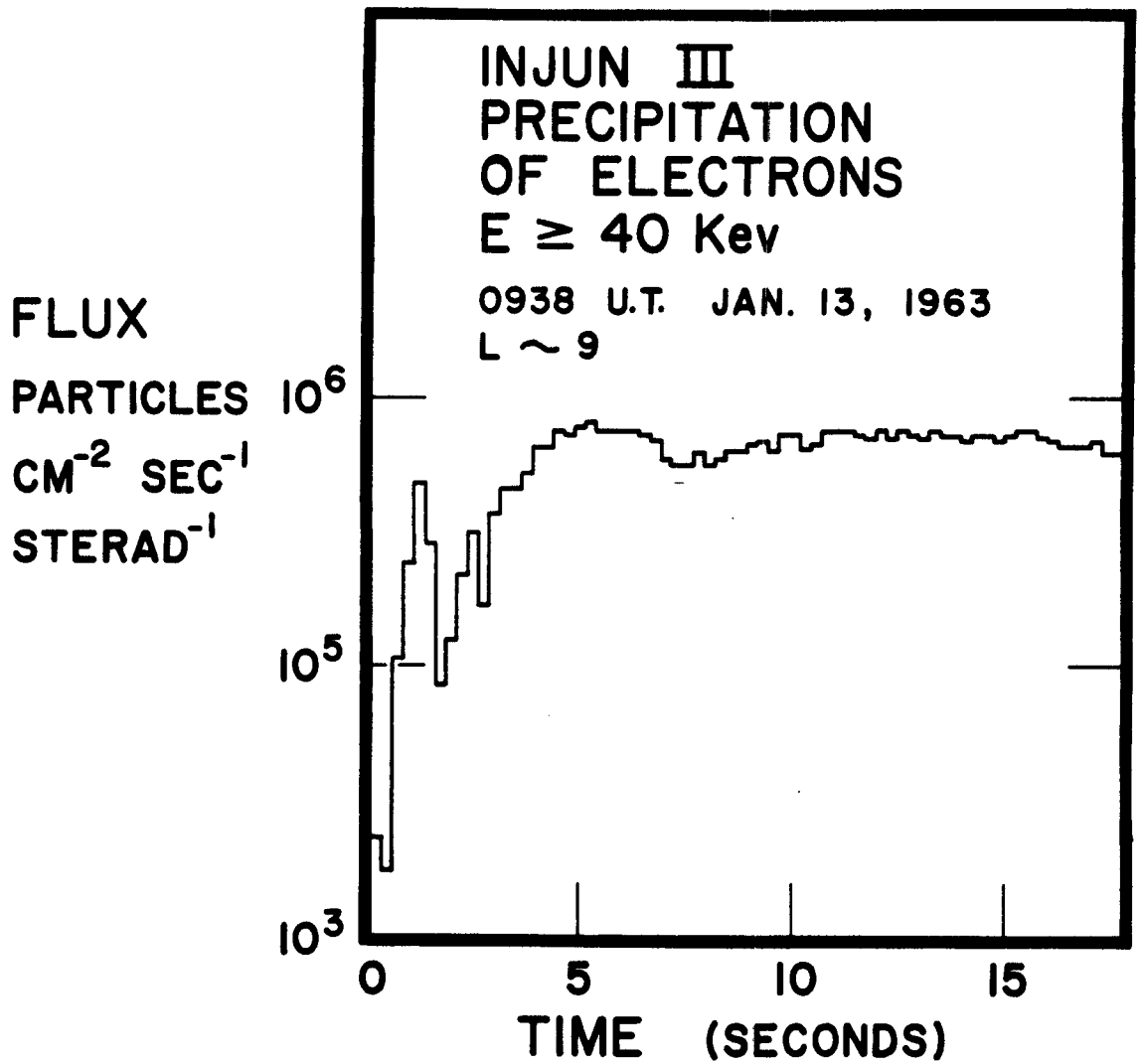
INJUN III
PRECIPITATION
OF ELECTRONS
E ≥ 40 Kev
0938 U.T. JAN. 13, 1963
L ~ 9
FLUX
PARTICLES
CM-2 SEC-1
STERAD-1
10^6
10^5
10^3
0
5
10
15
TIME (SECONDS)

Figure 17

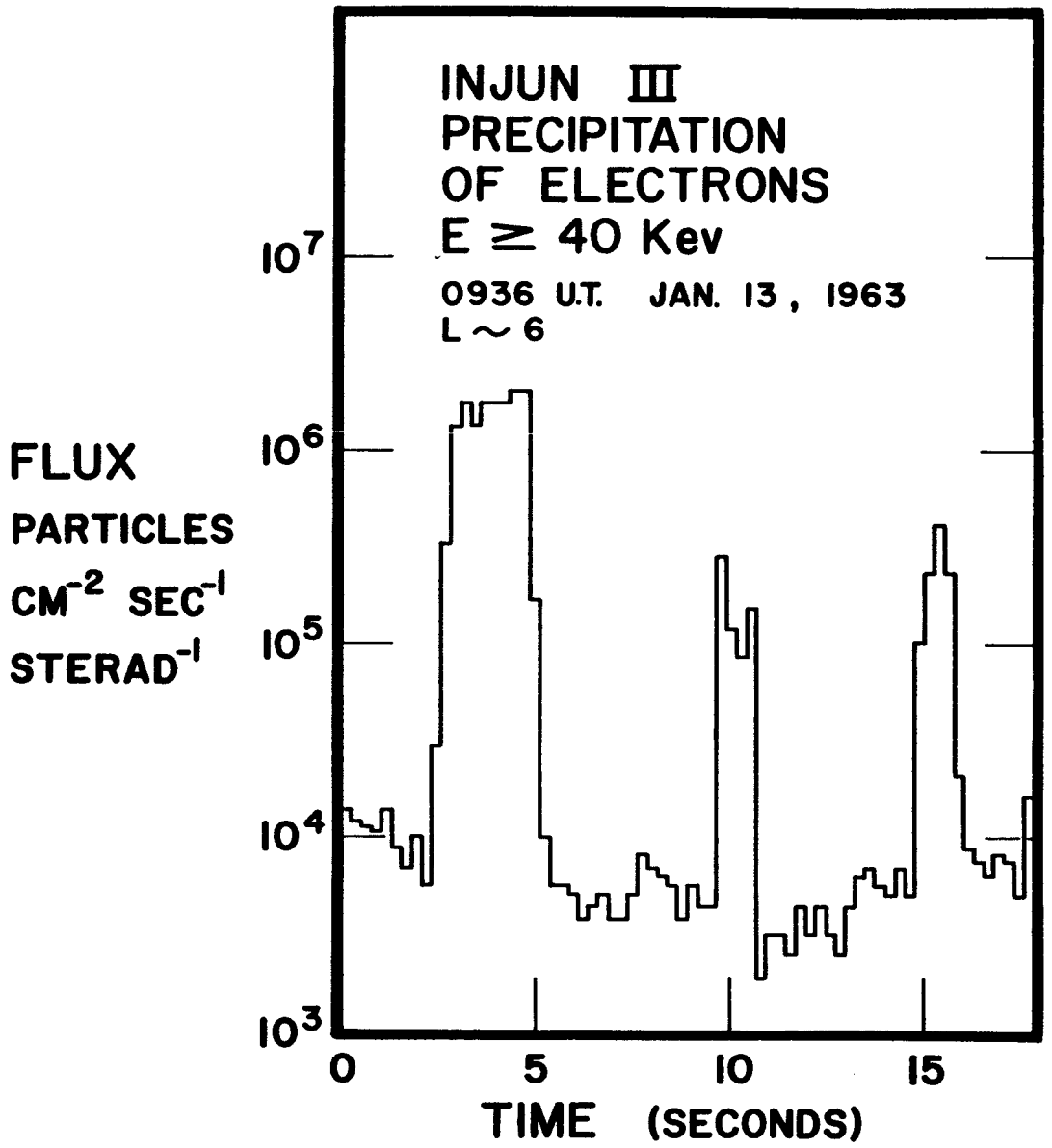
INJUN III
PRECIPITATION
OF ELECTRONS
E ≥ 40 Kev
0936 U.T. JAN. 13, 1963
L ~ 6
FLUX
PARTICLES
CM-2 SEC-1
STERAD-1
10^7
10^6
10^5
10^4
10^3
0
5
10
15
TIME (SECONDS)

Figure 18

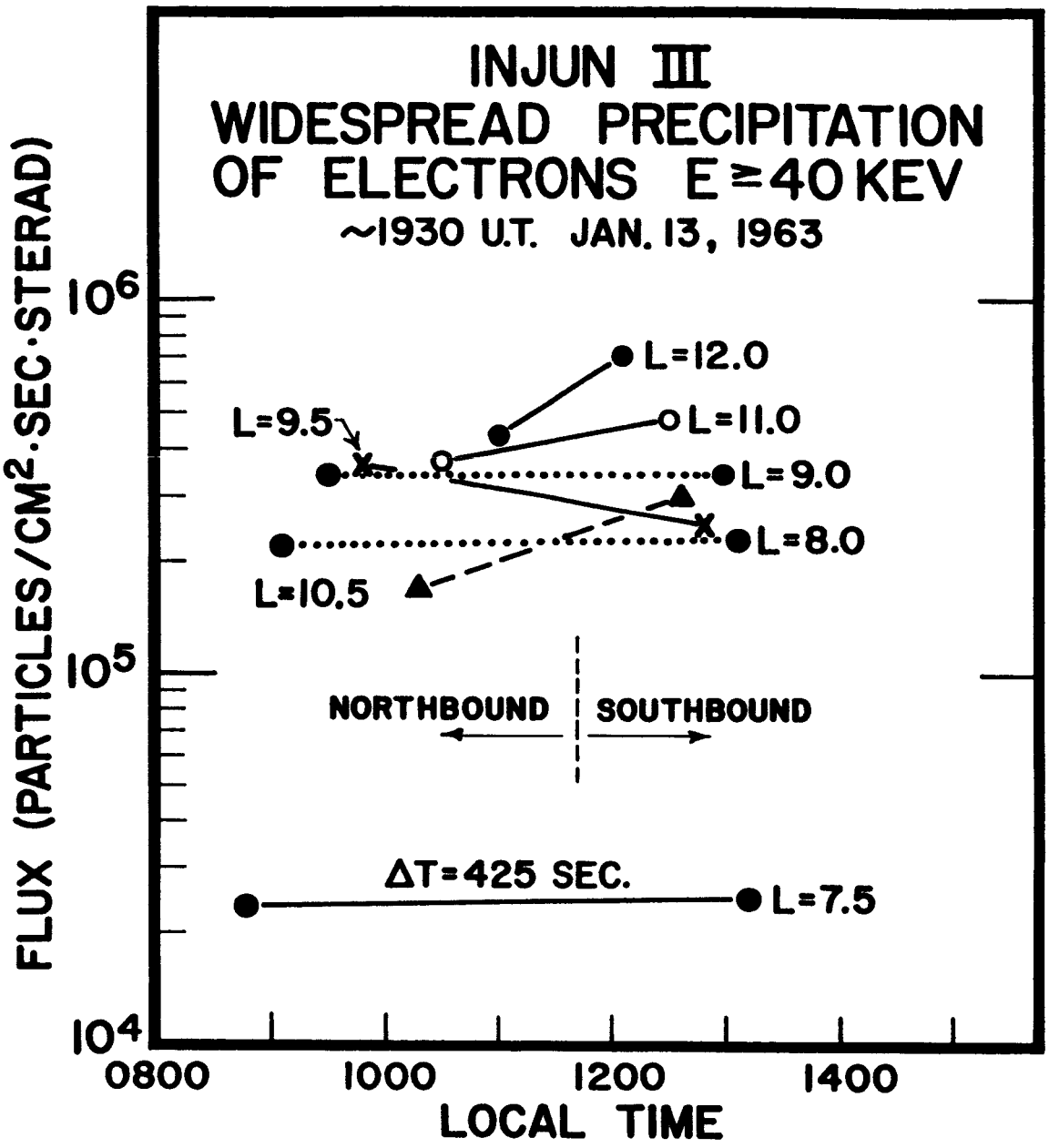
INJUN III
WIDESPREAD PRECIPITATION
OF ELECTRONS E ≥ 40 KEV
~1930 U.T. JAN. 13, 1963
FLUX (PARTICLES/CM².SEC·STERAD)
10⁶
10⁵
10⁴
L=12.0
L=11.0
L=9.5
L=9.0
L=8.0
L=10.5
NORTHBOUND
SOUTHBOUND
ΔT=425 SEC.
L=7.5
0800
1000
1200
1400
LOCAL TIME

Figure 19

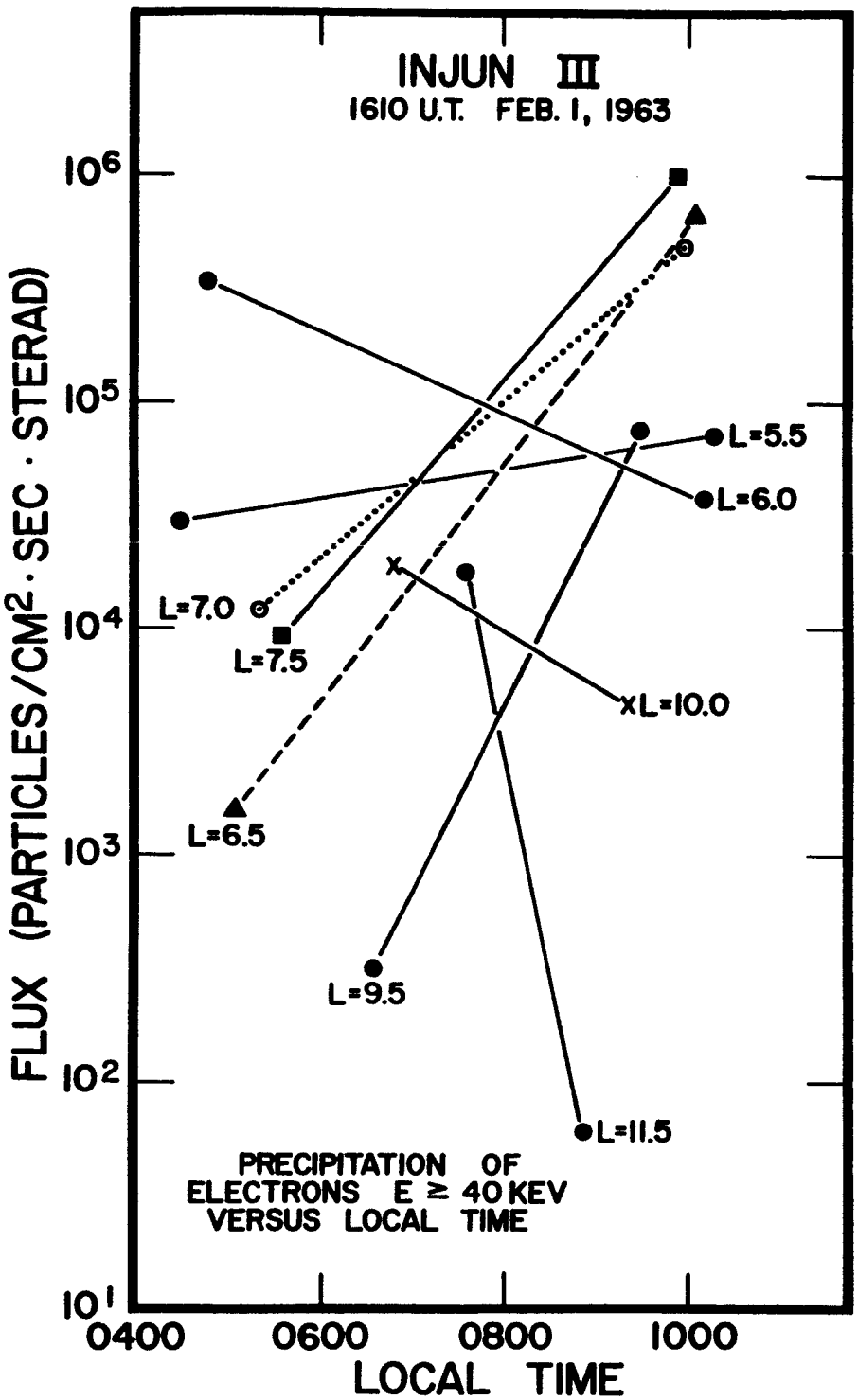
INJUN III
1610 U.T. FEB. 1, 1963
FLUX (PARTICLES/CM² · SEC · STERAD)
10⁶
10⁵
10⁴
10³
10²
10¹
L=5.5
L=6.0
L=7.0
L=7.5
L=10.0
L=6.5
L=9.5
L=11.5
PRECIPITATION OF
ELECTRONS E ≥ 40 KEV
VERSUS LOCAL TIME
0400
0600
0800
1000
LOCAL TIME

Figure 20

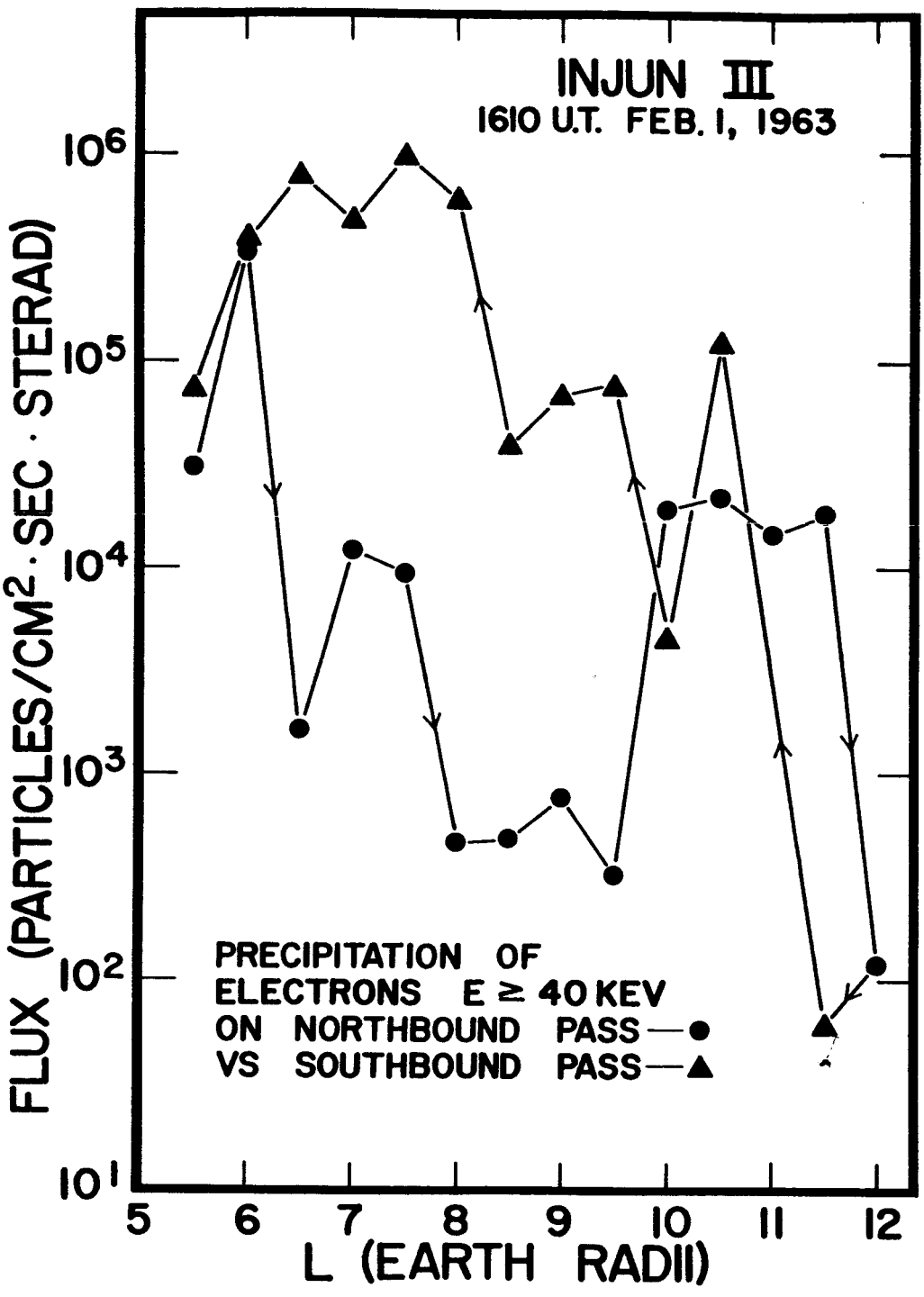
INJUN III
1610 U.T. FEB. 1, 1963
FLUX (PARTICLES/CM2 · SEC · STERAD)
10^6
10^5
10^4
10^3
10^2
10^1
PRECIPITATION OF
ELECTRONS E ≥ 40 KEV
ON NORTHBOUND PASS —●
VS SOUTHBOUND PASS —▲
5
6
7
8
9
10
11
12
L (EARTH RADII)

Figure 21

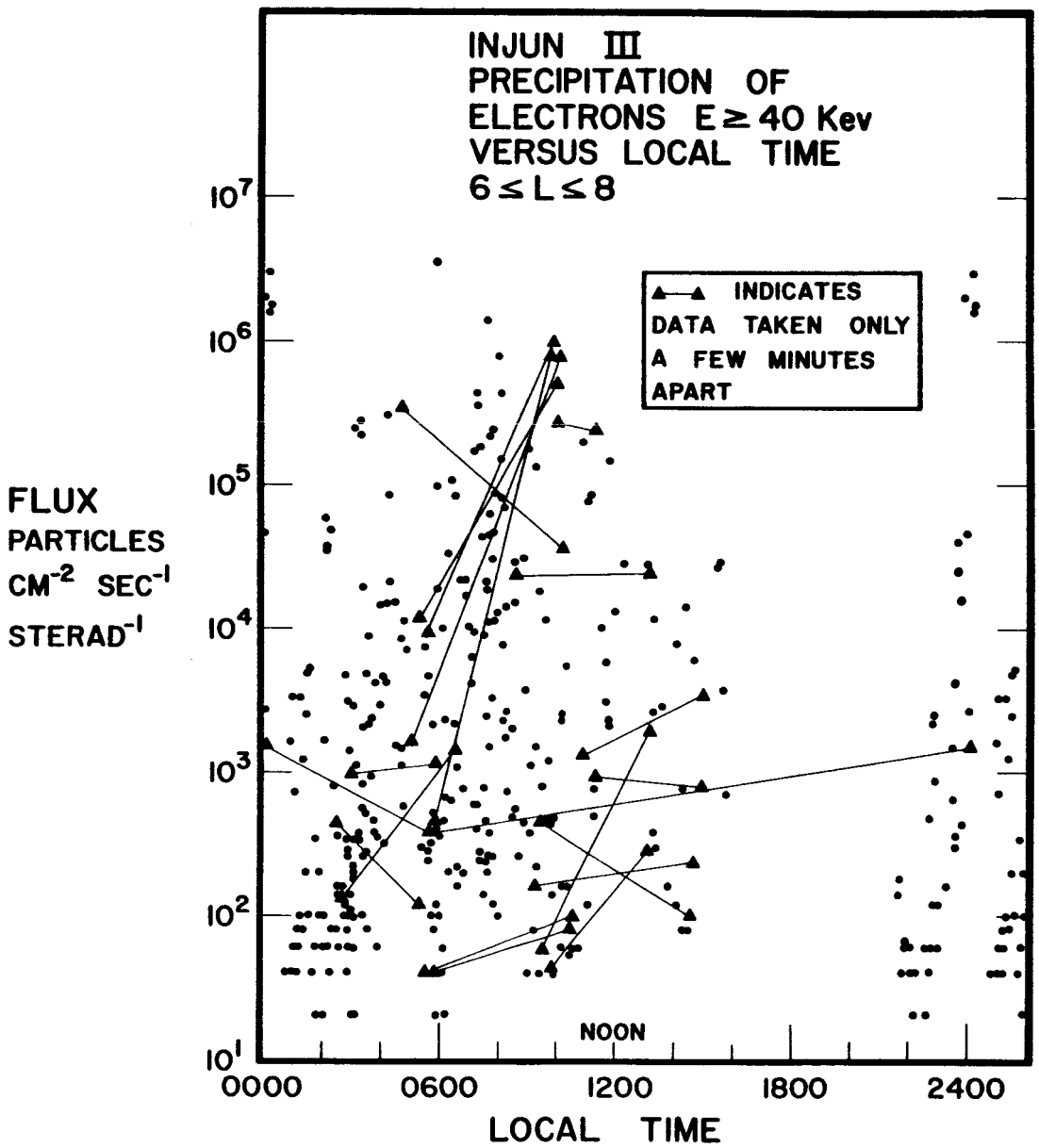
INJUN III
PRECIPITATION OF
ELECTRONS E ≥ 40 Kev
VERSUS LOCAL TIME
6 ≤ L ≤ 8
INDICATES
DATA TAKEN ONLY
A FEW MINUTES
APART
FLUX
PARTICLES
CM-2 SEC-1
STERAD-1
10^7
10^6
10^5
10^4
10^3
10^2
10^1
NOON
0000
0600
1200
1800
2400
LOCAL TIME

Figure 22

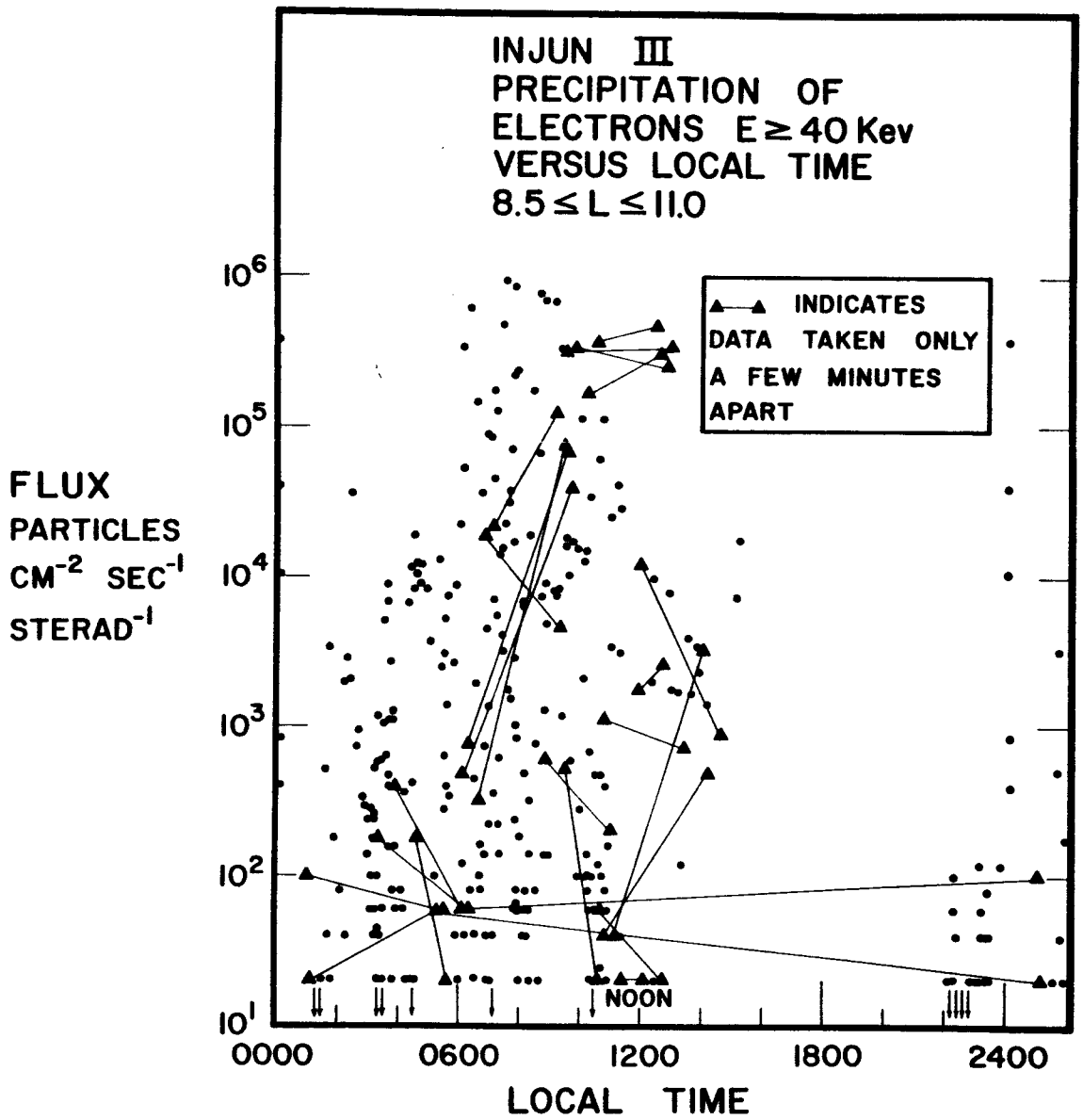
INJUN III
PRECIPITATION OF
ELECTRONS E ≥ 40 Kev
VERSUS LOCAL TIME
8.5 ≤ L ≤ 11.0
INDICATES
DATA TAKEN ONLY
A FEW MINUTES
APART
FLUX
PARTICLES
CM-2 SEC-1
STERAD-1
10^6
10^5
10^4
10^3
10^2
10^1
NOON
0000
0600
1200
1800
2400
LOCAL TIME

Figure 23

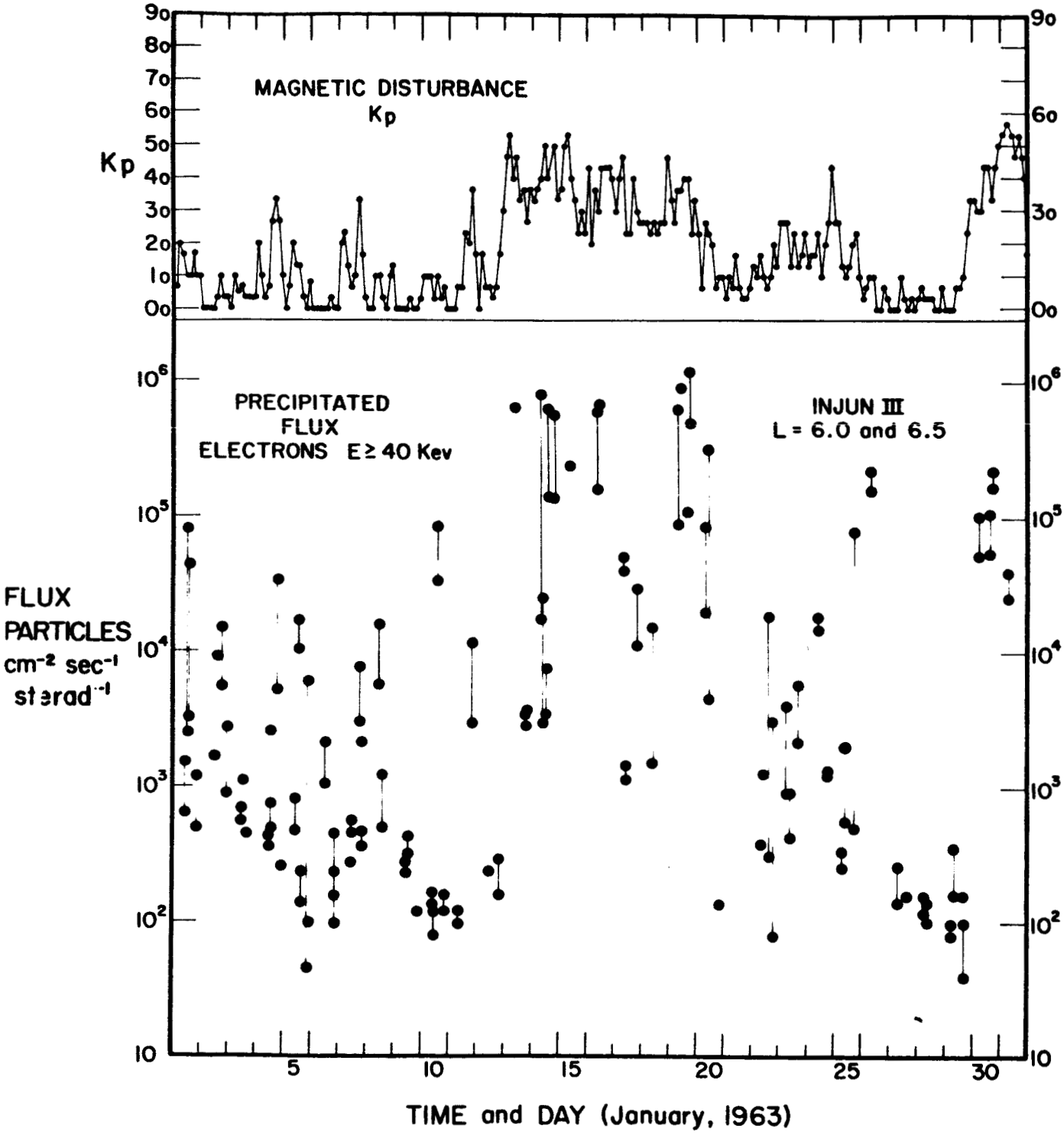
MAGNETIC DISTURBANCE
Kp
Kp
PRECIPITATED
FLUX
ELECTRONS E ≥ 40 Kev
INJUN III
L = 6.0 and 6.5
FLUX
PARTICLES
cm⁻² sec⁻¹
sterad⁻¹
TIME and DAY (January, 1963)

Figure 24

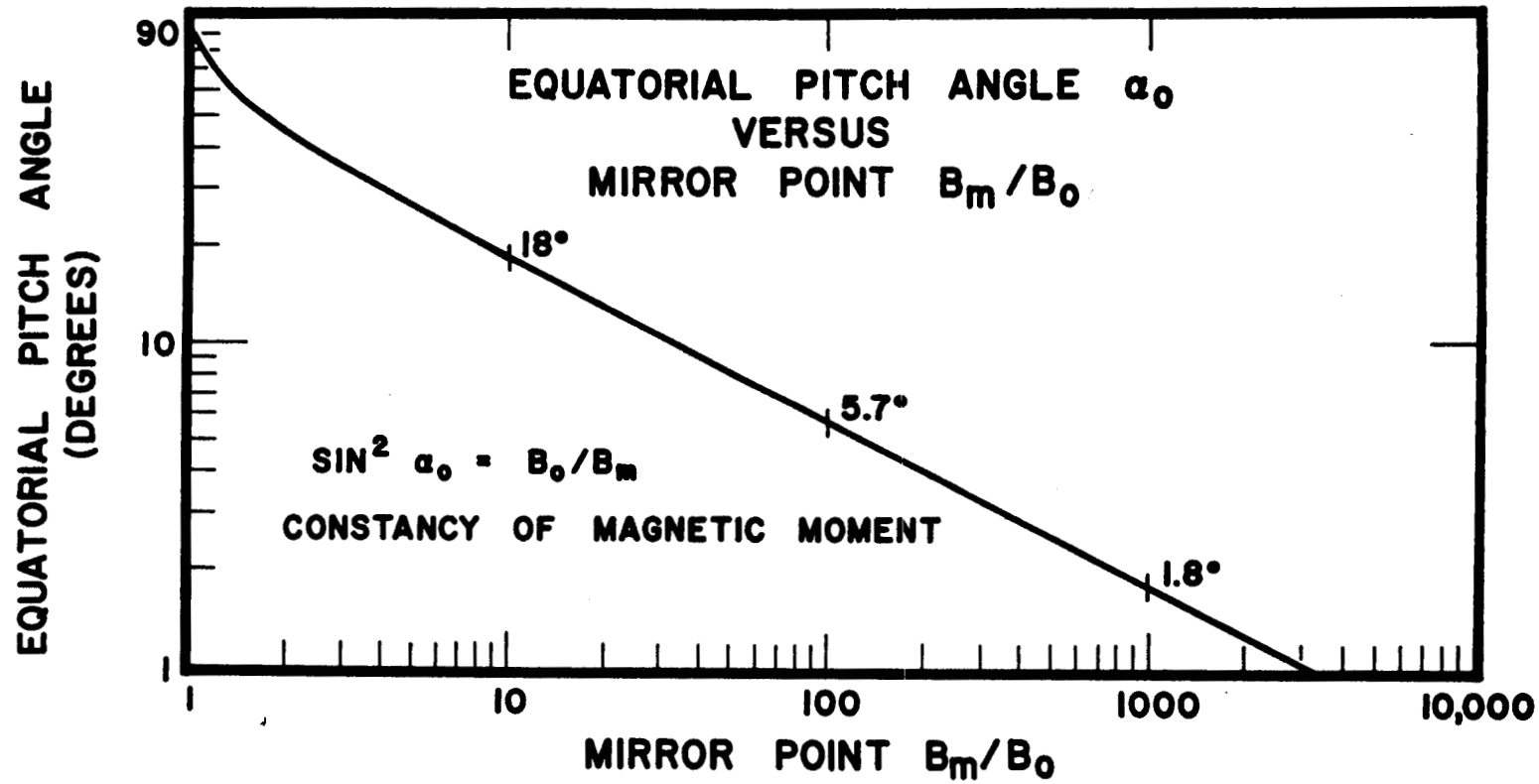
EQUATORIAL PITCH ANGLE (DEGREES)
90
10
1
EQUATORIAL PITCH ANGLE α_0
VERSUS
MIRROR POINT B_m/B_0
18°
5.7°
1.8°
$\sin^2 \alpha_0 = B_0/B_m$
CONSTANCY OF MAGNETIC MOMENT
1
10
100
1000
10,000
MIRROR POINT B_m/B_0

Figure 25